This project has received funding from the European Union's Horizon 2020
research and innovation programme under grant agreement No 869226

Report on catchment-scale spatially distributed models for the 6 European focal DRNs

Document authors:	Annika Künne (FSU), Louise Mimeau (INRAE), Flora Branger (INRAE), Sven Kralisch (FSU)
Document contributors:	Alexandre Devers, Claire Lauvernet, Jean-Philippe Vidal, Thibault Datry (INRAE)

Abstract

Intermittent rivers and ephemeral streams (IRES) account for more than half of the world's river networks and are considered to increase under climate change and growing anthropogenic water use. However, the hydrological mechanisms that control the spatio-temporal flow patterns in IRES and their effects on the expansion and contraction of stream segments are not fully understood. Aiming to overcome this problem, DRYvER developed a hybrid hydrological modeling approach to simulate daily flow conditions and provide flow intermittence indicators in 6 European Drying River Networks (DRNs).

The JAMS/J2000 process-based hydrological model forced with the ERA5-land reanalysis is used to simulate daily discharges at high spatial resolution, which includes the scale of small reaches (about 50 ha catchment size). As the JAMS/J2000 does not allow to reproduce accurately the periods with no flow, a Random Forest classification model (RF) was used to predict the flow condition (dry or flowing) at the reach scale in the DRNs, using hydrological variables simulated with JAMS/J2000 as explanatory variables, and observed flow intermittence data (e.g. data from field measurements, citizens science application) to train the RF model.

Results show that the hybrid hydrological modeling approach (JAMS/J2000 and RF) enables to reproduce accurately the spatio-temporal patterns of flow intermittence in the Albarine (France), Bukkosdi (Hungary), Lepsämänjoki (Finland), and Velička (Czech Republic) DRNs. Additional observed flow intermittence data would be needed in the Genal (Spain) DRN in order to improve the simulation results. The prediction of flow conditions could not be produced for the Butižnica (Croatia) DRN due to a lack of observed flow intermittence data.

Keywords: hydrological modeling, Drying River Networks, flow intermittence, Machine Learning

Information Table

PROJECT INFORMATION	
PROJECT ID	**869226**
PROJECT FULL TITLE	**Securing biodiversity, functional integrity and ecosystem services in DRYing riVER networks**
PROJECT ACRONYM	**DRYvER**
FUNDING SCHEME	**Horizon Europe**
START DATE OF THE PROJECT	**1st September 2020**
DURATION	**48 months**
CALL IDENTIFIER	**LC-CLA-06-2019**

DELIVERABLE INFORMATION	
DELIVERABLE No AND TITLE	D1.2 Report on catchment-scale spatially distributed models for the 6 European focal DRNs
TYPE OF DELIVERABLE [1]	R
DISSEMINATION LEVEL [2]	PU
BENEFICIARY NUMBER AND NAME	2 - FSU
AUTHORS	Annika Künne, Louise Mimeau, Flora Branger, Sven Kralisch
CONTRIBUTORS	Alexandre Devers, Claire Lauvernet, Jean-Philippe Vidal, Thibault Datry (INRAE)
WORK PACKAGE No	1
WORK PACKAGE LEADER WP LEADER VALIDATION DATE	Jean-Philippe Vidal – 31.10.2022
COORDINATOR VALIDATION DATE	Thibault Datry

[1] **Use one of the following codes:**
R=Document, report (excluding the periodic and final reports)
DEM=Demonstrator, pilot, prototype, plan designs
DEC=Websites, patents filing,press & media actions, videos, etc.
OTHER=Software, technical diagram, etc.
ORDP : Open Research Data Pilot

[2] **Use one of the following codes:**
PU=Public, fully open, e.g. web
CO=Confidential, restricted under conditions set out in Model Grant Agreement
CI=Classified, information as referred to in Commission Decision 2001/844/EC.

Table of contents

1 Introduction

1.1 Background

Currently, more than half of the world's river channels are considered as intermittent rivers and ephemeral streams (IRES), that recurrently cease flow and/or dry (Datry et al. 2021; Messager et al. 2021); Figure 1.1). Even though IRES can occur naturally across every river network, they are expanding in time and space, mainly due to human water use and climate change. Our limited knowledge about the expansion and contraction of river networks as well as hydrological process interactions restrict model implementations as well as confines future projections (van Meerveld et al. 2019).

DRYvER's multi model approach aims to simulate hydrological, biological, and biogeochemical processes to assess biodiversity, ecosystem functions, and services. These predictions and future projections are therefore constrained by the performance of the hydrological models at the catchment scale.

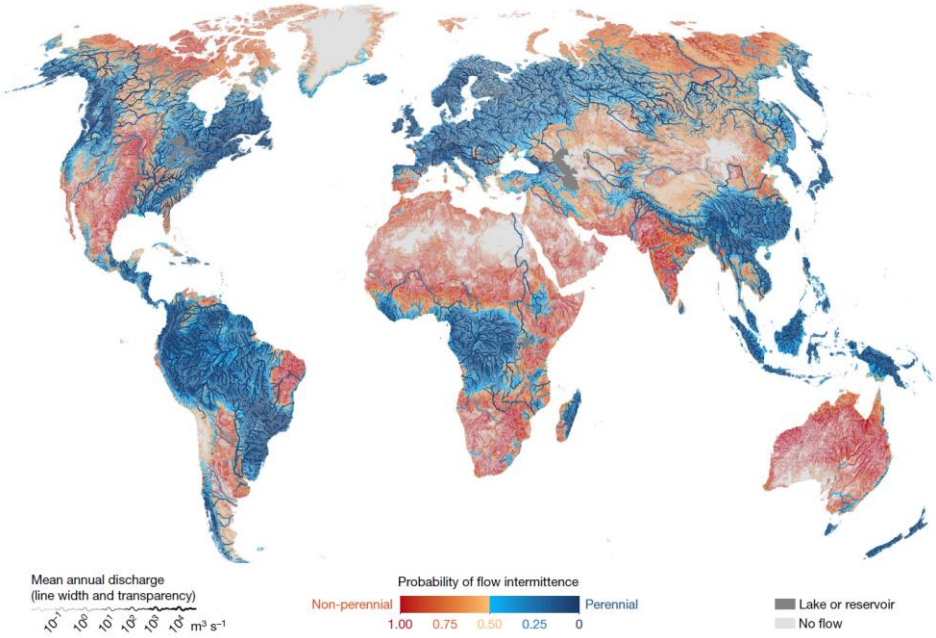

Figure 1.1: Probability of flow intermittence at the global scale (Messager et al. 2021)

1.2 Objectives

The objective of Task 1.1 is to provide flow intermittence patterns for the six EU focal Drying River Networks (DRNs), for present conditions and future climate scenarios, taking into account human influences (e.g. abstraction, reservoirs) on hydrological process dynamics of the DRNs. The aim is to implement process-based spatially distributed hydrological models – based on the JAMS/J2000 modeling system at daily time-steps (ST 1.1.1). Besides, to use observed data of the states of flow within the focal DRNs to validate the models and, if necessary, adapt the modeling strategy to predict flow intermittence. The developed models for the focal DRNs in Hungary, Spain, Croatia, France, Czech Republic, and Finland can then be used to calculate indicators of flow intermittence, such as the presence/absence and frequency of drying in recent decades and under projected climate scenarios in the future (D1.1).

This report aims to describe the model setups, calibration and validation as well as to show results and updated datasets on flow intermittence at present time.

2 Methods

Within WP1 task 1.1, INRAE and FSU jointly developed process-based spatially distributed hydrological models for the six European focal DRNs, which are based on the JAMS/J2000 modeling system/hydrological model, running at a daily time-step (ST 1.1.1). For the development of the hydrological models, FSU took charge of three European DRNs, located in Spain, Czech Republic, and Croatia and INRAE the DRNs located in France, Hungary, and Finland, but worked constantly together to develop a joint methodology and harmonized datasets. The first task was the collection, analysis, and selection of required data to set up the physical-based models. In the second step, these models were calibrated and validated using long-term (20 years) streamflow data. To capture the spatio-temporal dynamics of observed flow states, the physically-based hydrological model was coupled with a stochastic model, to use the model outputs and physical information to train a Machine Learning (ML), Random Forest (RF) model with the flow state observations. Following, these steps are described in detail.

2.1 Spatial and temporal data acquisition and analysis for model development

Harmonized databases were established containing hydro-climatic time-series of the last 20 years and spatial topographical, pedo-lithological and land use land cover (LULC) data.

2.1.1 Temporal data (hydroclimatic time series)

The temporal data used for the modeling needed to fulfill certain requirements. The most important one was to be up-to-date to integrate the latest observations from the field teams. Usually, locally observed data is used to ensure the most precise data basis. However, for meteorological data, it was not possible for all DRNs to regularly update the data every few months. For that reason, reanalysis and modeled meteorological data products were tested, selected, and used to force the hydrological models. These products were then compared among each other and to the measured data (Mimeau et al. 2022).

Therefore, at first, a database was established, which contains available measured discharge and meteorological parameters. It is hosted by FSU and available online (http://leutra.geogr.uni-jena.de/DRYvER). Currently, 371 meteorological and gauging stations are available, which comprise 1030 time series (Figure 2.1) and can be used by the project consortium. Metadata and references for all measured discharge used in this study can be found in this dataset.

Another requirement for the modeled and reanalysis data was that the available meteorological variables should also contain the same variables and formats that are available in the climate model data to guarantee a seamless alignment. This especially addresses the calculation of evapotranspiration. The final data fulfilling these requirements and thus, selected to force the models were the ERA5-Land data (Muñoz-Sabater et al. 2021). The following hourly ERA5-Land climate variables were used to compute the reference evapotranspiration using the Penman-Monteith equation (Allen et al. 1998): 2m air temperature (°C), 2m dew point temperature (°C), 2m relative humidity (%), 10m u and v wind speed components (m/s, incoming solar radiation (W/m²), incoming thermal radiation (W/m²), and surface pressure (Pa). Hourly ERA5-Land precipitation, air temperature

and computed reference evapotranspiration were then aggregated at daily time step to be used as climate forcing data in the hydrological model.

Additionally, daily discharge data for the six DRNs was required for at least 20 years to calibrate and validate the models at as many gauging stations as possible and at least at the outlet of the small and large catchment. The reason behind, was to capture the magnitude and frequency of the hydrological process dynamics in time and space. For example, to cover the temporal variability and extreme events, but also changes in the transition time from upstream to downstream parts in the catchment. The available and used discharge stations, which were fulfilling these requirements are listed in Table 2.1.

Table 2.1: *Available discharge data*

DRN	gauging stations	time series (average length in years)	stations with inhomogeneity	used
Guadiaro/Genal	4	20	2	3
Krka/Butižnica	3	20	1	2
Morava/Velička	9	41	0	9
Fekete/Bukkosdi	22	25	5	17
Ain/Albarine	25	49	2	23
Vantaanjoki/Lepsämänjoki	11	47	4	7

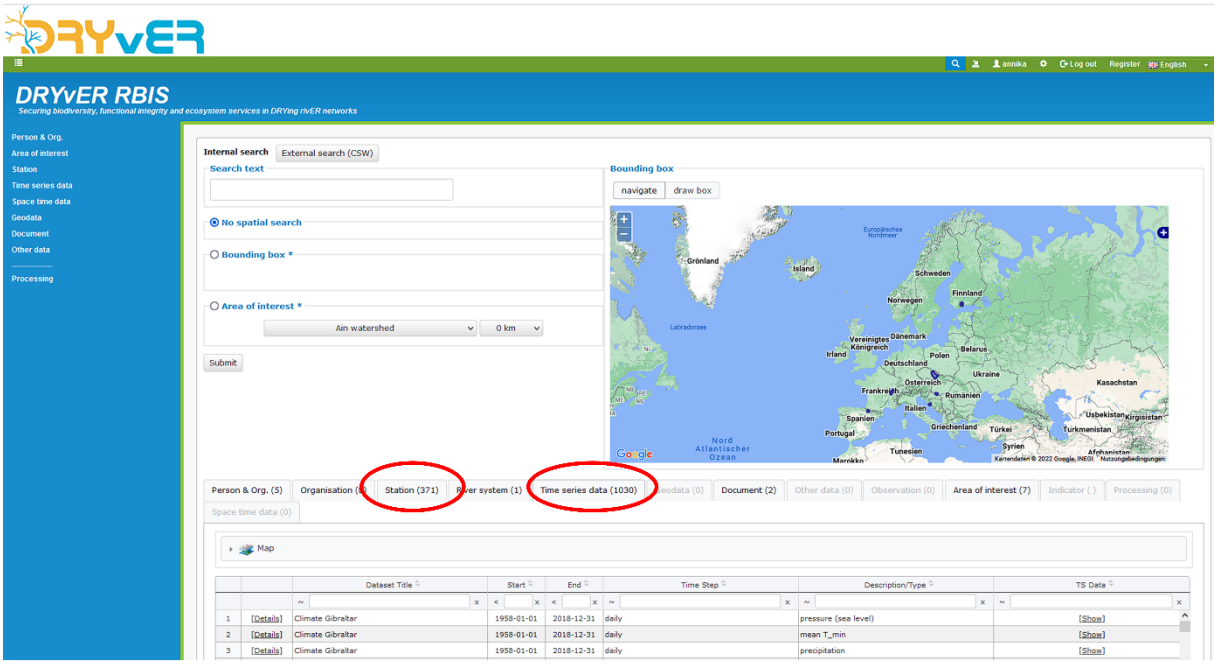

Figure 2.1: DRYvER River Basin Information System

Besides, observed snow data was used to calibrate and validate JAMS/J2000's performance of modeling snow processes. For that purpose, the catchment's fractional snow cover area (fSCA) was used from the MOD10A2 dataset (Hall and Riggs 2016; section 2.3.1)

2.1.2 Spatial data (as basis for the modeling entities)

The spatial data is key to delineate the modeling entities and deriving bio-physical information for the mathematical calculation of hydrological processes.

For the delineation of modeling entities, the concept of Hydrological Response Units (HRUs) and stream segments (reaches) as well as topological routing according to Flügel (1996) and Pfennig et al. (2009) was used (Figure 2.2). The topological routing scheme allows the calculation of water transfer from one HRU to another until the reach and further along the reaches until the basin outlet (Pfennig et al. 2009), enabling to simulate different flow conditions at the reach level. For DRYvER, special attention was drawn to the replication of the river networks to address the replication of both, i) the original river network with the sampling points of the DRN teams and ii) a high spatial resolution to assure that models are able to simulate hydrological dynamics at the resolution required by the other work packages. For that purpose, reference river networks provided by the DRN leaders were used to validate the synthetic river networks, which are constrained by the DEMs Table 2.2 used for each DRN.

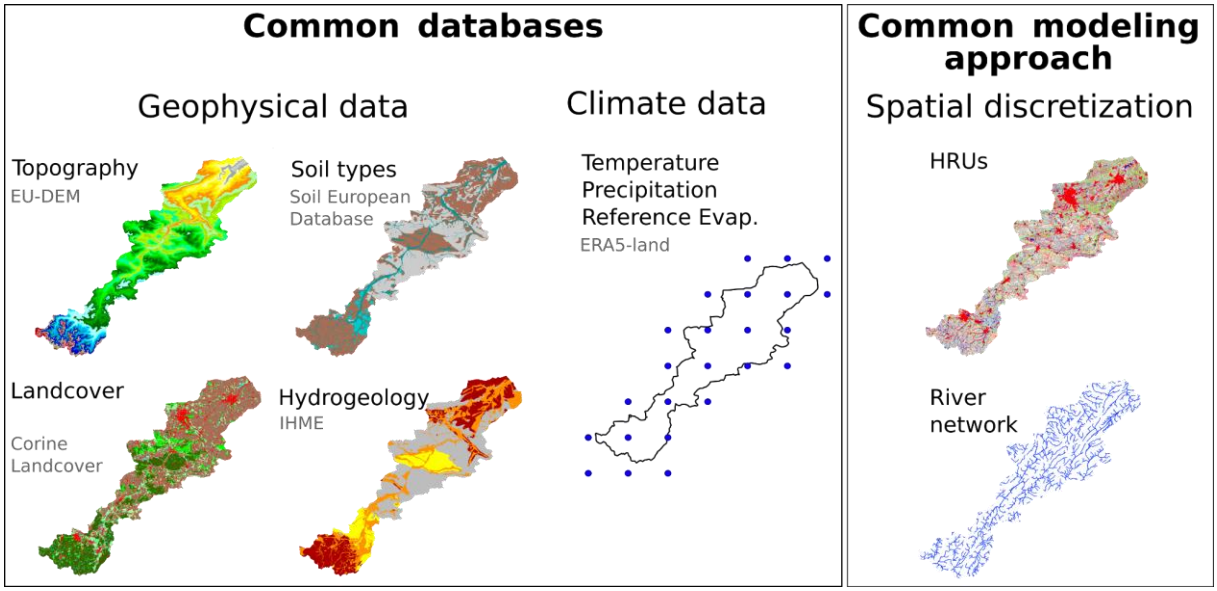

Figure 2.2: Harmonized hydrological data used to generate the modeling entities (Hydrological Response Units; HRUs and reaches)

Besides, bio-physical information of these spatial classes was used to calculate plant-based processes, such as evapotranspiration, soil water processes, e.g. infiltration and groundwater processes, such as groundwater recharge and based on these processes the discharge. Besides, topographic information, such as slope and aspect are needed to replicate the flow topology (section 2.2). Additionally, these classes of e.g. a specific soil type or land use class are attributed with physical (e.g. field capacity) or biological (e.g. root depth) information, which is needed to model the associated processes. If available, European data products were used to establish a common spatial database and select classes, which are hydrologically relevant to assure transparency. The following data sources were used:

- **Topography**: Digital Elevation Models (DEMs) were selected based on their availability and quality in representing the river network and sampling reaches of WP2 provided by the DRN team leaders. Besides, the area of certain catchments restricted the use of a high-resolution DEM due to calculation problems. This was for example the case for the Morava DRN, which covers the largest area among the six DRNs (A ≈ 9,400 km²). The DEMs used for the specific DRNs are listed in Table 2.2.
- **Soil**: Soil classes were adapted using the European Soil Database v2.0 (European Commission; (Panagos et al. 2012). Physical parameters were also used from the European Soil Database v2.0 (field capacity, saturated water content, depth to rock). In Spain, texture and bulk density

data was used from soil profiles (Llorente et al. 2018) for the calculation of parameters using pedotransfer functions (Ad-hoc-AG Boden 2005; FAO 2006; Table 2.2).

- **LULC**: Corine Land Cover (CLC) 2012, Version 2020_20u1 Level 3 (44 classes) was used (Copernicus Land Monitoring Service 2020) to establish the LULC classes. Parameters, such as albedo, crop coefficients, LAI, root depth, and impervious fraction area, were adapted to local conditions from different sources (Allen et al. 1998; Krause 2001; Ludwig and Bremicker 2006; Neitsch et al. 2011; Faroux et al. 2013; Table 2.2).
- **Hydrogeology**: IHME1500 – International Hydrogeological Map of Europe (aquifer and lithology layers) was used to establish the classes for all DRNs (BGR 2013). Besides, physical parameters were used from the literature (Andreas and Duscher 2019) to parameterize the models to calculate groundwater flow for the Krka (Croatia), Guadiaro (Spain), and Morava (Czech Republic) DRNs (Table 2.2).

Table 2.2: References for the digital elevation models used to generate Hydrological Response Units (HRUs) and topological routing of water pathways as well as pre-determined spatially distributed parameter values

<table>
<tr><th rowspan="2">Type</th><th rowspan="2">Parameter</th><th colspan="5">Country DRN</th></tr>
<tr><th>France, Hungary</th><th>Finland</th><th>Croatia</th><th>Czech Republic</th><th>Spain</th></tr>
<tr><td rowspan="2">Topography [resolution]</td><td>Slope</td><td rowspan="2">EU-DEM v1.1 (Copernicus Land Monitoring Service 2016) [25 m]</td><td rowspan="2">10 m DEM Finland (National Land Survey of Finland) [10 m]</td><td rowspan="2">EU-DEM v1.1 (Copernicus Land Monitoring Service 2016) [25 m]</td><td rowspan="2">Shuttle Radar Topography (SRTM30; U.S. Geological Survey 2015) [30 m]</td><td rowspan="2">MDE de Andalucía (Portal Ambiental de Andalucía. 2010) [10 m]</td></tr>
<tr><td>Aspect</td></tr>
<tr><td rowspan="3">Soil</td><td>Field capacity</td><td colspan="4" rowspan="3">European Soil Database v2.0 (Panagos et al. 2012)
(Air capacity = field capacity - saturated water content)</td><td rowspan="3">Llorente et al. 2018, Boden 2005; FAO 2006</td></tr>
<tr><td>Air capacity</td></tr>
<tr><td>Soil depth</td></tr>
<tr><td rowspan="5">LULC</td><td>Albedo</td><td colspan="5">(Ludwig and Bremicker 2006)</td></tr>
<tr><td>Monthly crop coefficient</td><td colspan="5">FAO (Allen et al. 1998)</td></tr>
<tr><td>Monthly Leaf area index</td><td colspan="5">ECOCLIMAP II (Faroux et al. 2013)</td></tr>
<tr><td>Root depth</td><td colspan="5">(Ludwig and Bremicker 2006)</td></tr>
<tr><td>Impervious-ness</td><td colspan="5">Percentage of sealed area within each LULC class Corine Land Cover (CLC) 2012, Version 2020_20u1 Level 3 (Copernicus Land Monitoring Service 2020)</td></tr>
<tr><td rowspan="2">Hydro-geology</td><td>Storage capacity</td><td colspan="2">calibrated</td><td colspan="3">BGR 2013; Andreas and Duscher 2019</td></tr>
<tr><td>Storage or recession coefficient</td><td colspan="5">calibrated</td></tr>
</table>

2.1.3 Flow intermittence data

In order to validate the model's ability of simulating flow intermittence at the reach level multiple data sources of flow observations were used, which stem from the:

- DRYRivERS smartphone application developed in DRYvER (https://www.dryver.eu/citizen-science/introduction; all DRNs)
- crowdwater smartphone application (https://crowdwater.ch/en/data/; France, Hungary, Finland)
- ONDE network (Observatoire National des Etiages, https://onde.eaufrance.fr; France)
- photo traps installed in DRYvER (France, Finland)
- temperature and conductivity sensors installed in DRYvER (Czech Republic)
- water level and discharge sensors installed in DRYvER (Czech Republic)
- discharge daily time series from gauging stations (all DRNs)

These data sources were available either as disconnected points in time and space, recurrent observations at the sampling sites, or time series of daily data over periods ranging from a few months to several years.

For this deliverable flow intermittence data until 2021-30-09 was used (Figure 2.3 and Table 2.3). Until the end of the project, the datasets of flow intermittence will be updated to consider new observations (e.g. observations for the year 2022, photo traps data in the Bukkosdi catchment, water temperature data in the Albarine, Bukkosdi, Genal, Lepsämänjoki, and Velička DRNs).

Table 2.3: Flow observations in the studied DRNs (from 2018-01-01 to 2021-12-31)

Catchment	Dataset	Number of observations	Number of sites	Length of river network with observed data [%]
Albarine	DryRivers	120	57	12.6
	CrowdWater	215	32	8.2
	Photo traps	5093	10	2.5
	ONDE	54	3	0.7
	Gauging stations	1462	2	0.5
Bukkosdi	DryRivers	183	37	11.2
	CrowdWater	33	26	7.8
	Gauging stations	2500	6	0.5
Lepsämänjoki	DryRivers	24	17	5
	CrowdWater	4	4	2.2
	Photo traps	816	8	2.8
	Gauging stations	877	1	0.1
Genal	DryRivers	72	33	12.2
	Gauging stations	1387	1	0.3
Butižnica	DryRivers	21	21	4.3
	Gauging stations	1096	1	0.05
Velička	DryRivers	351	20	62.5
	Gauging stations	1460	2	1.7
	Water level and discharge loggers	5117	7	8.3
	Temperature/ Conductivity loggers	5403	20	23

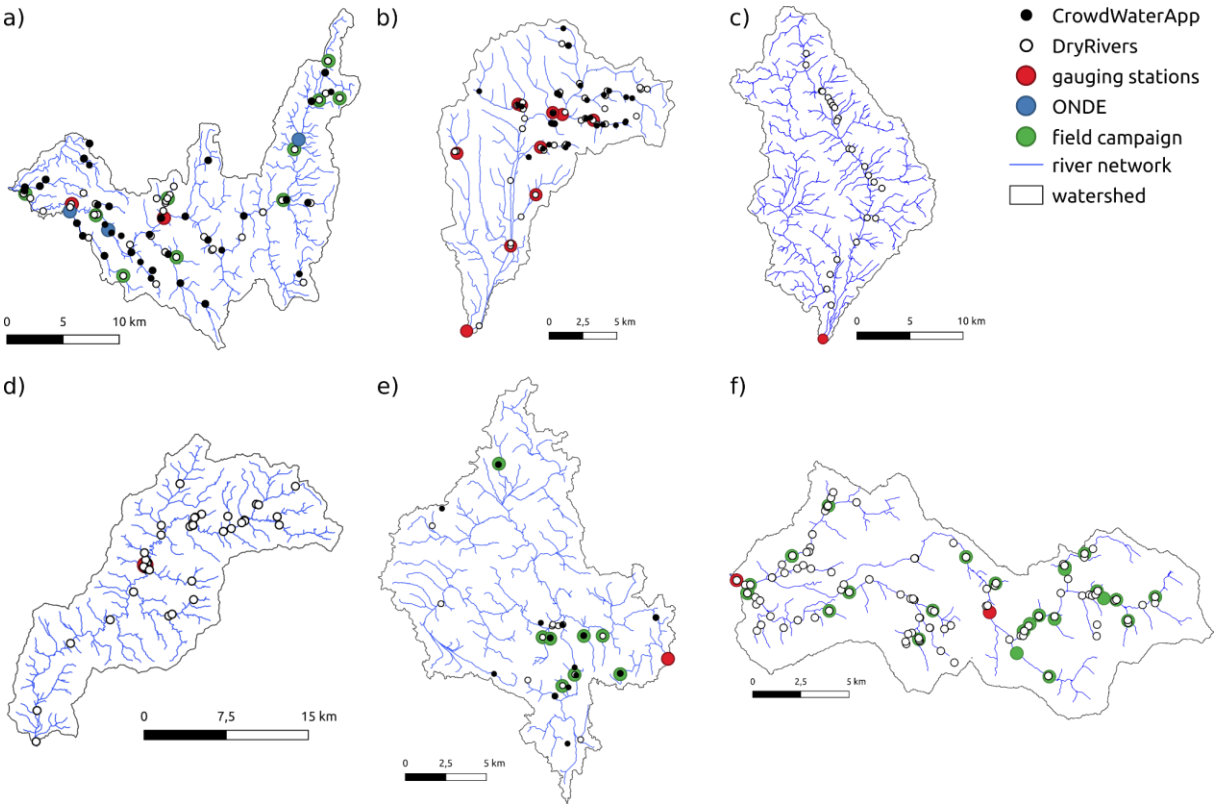

Figure 2.3: Location of flow observations in the a) Albarine (France), b) Bukkosdi (Hungary), c) Butižnica (Croatia), d) Genal (Spain), e) Lepsämänjoki (Finland), and f) Velička DRNs. Different sources of data are reported for each catchment: crowdsourced observations (from the CrowdWater app in black and from the DryRivers app in white), hydrological stations (gauging stations in red and ONDE stations in blue for the Albarine, France only) and field campaign observations (photo traps, water level loggers, water temperature loggers, conductivity loggers).

2.2 Model structure

The models for the six DRNs were developed in a joint effort by INRAE and FSU using the process-oriented model J2000 (Krause 2001, 2002) together with the modular object oriented modeling system JAMS (Kralisch and Krause 2006) considering both process dynamics at the reach and HRU level to account for surface, sub-surface, and groundwater flow from hillslopes into the stream and along stream segments until the outlet. From climate forcing data, JAMS/J2000 simulates plant-related ecohydrological processes as well as the soil water balance and groundwater processes at the HRU level and based on that different runoff components at the reach level (Figure 2.4).

Due to the modular design of the underlying JAMS modeling framework (Kralisch and Krause 2006), the models were harmonized with respect to the aims of DRYvER and the European databases, which allowed a transparent and reproducible modeling structure and process. For that purpose, modifications from the standard J2000 hydrological model were made for DRYvER using the evapotranspiration module from Branger et al. (2016) to compute potential evapotranspiration using the reference evapotranspiration and spatially distributed crop coefficients. Besides, the adapted J2000 snow module by Gouttevin et al. (2017) was used.

Additionally, adaptations were made to account for anthropogenic influences in the French DRN to account for Vouglans hydroelectric dam. The dam is at the origin of an artificial lake with a capacity of 605 Mm^3, and is causing a change in the hydrological regime of the Ain river downstream of the reservoir. A module representing the Vouglans reservoir was added to the JAMS/J2000 model. This module either stores water from the reach into the reservoir or releases water from the reservoir into the reach according to an operational instruction (Branger et al. 2016) provided as input to the model.

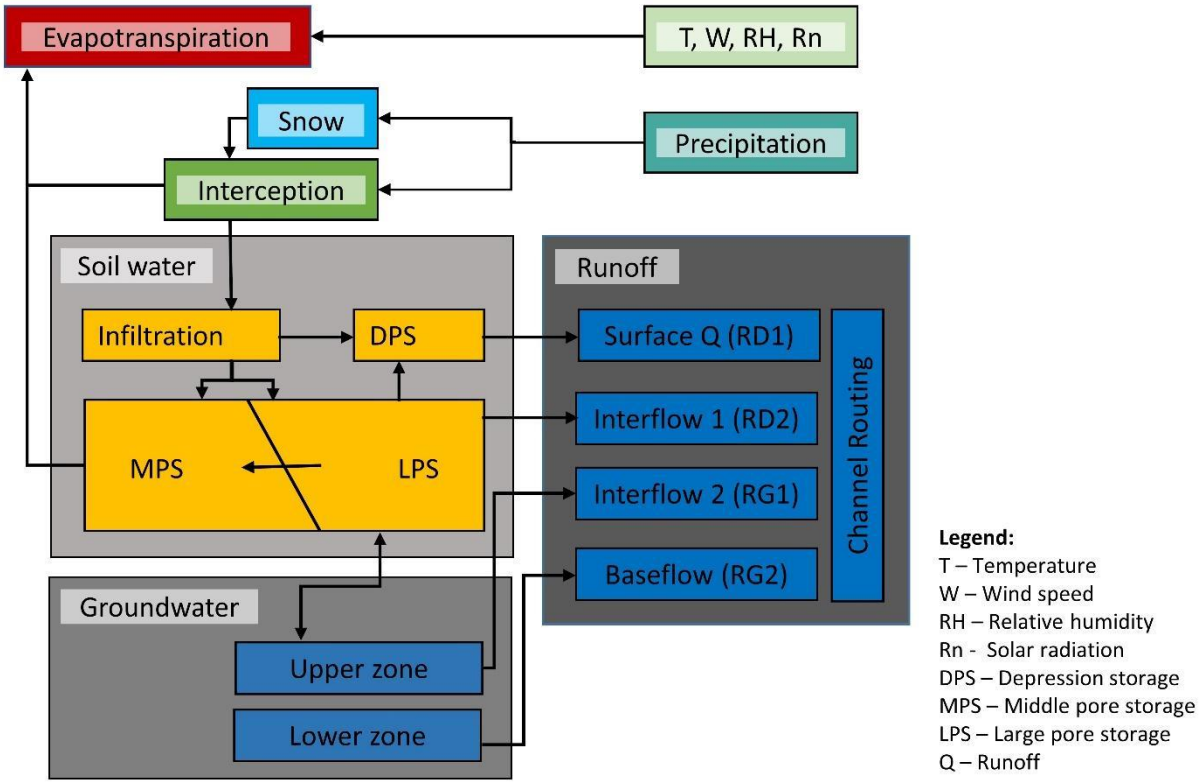

Figure 2.4: Schematic representation of the hydrological processes modeled in JAMS/J2000 at the HRU and reach level according to Krause (2001), Figure adapted from (Watson et al. 2020)

2.3 Model calibration

Several techniques were used to calibrate the hydrological models for the six pilot-watersheds to find the optimal models and gain a wider perspective of the model's sensitivity, parameter interactions, and uncertainty by investigating hydrological process patterns via e.g. hydrological signatures.

2.3.1 Calibration of Snow Parameters

Snow parameters were calibrated separately by comparing the simulated snow cover with the catchments' fractional snow cover area from MODIS10A2 datasets using the Kling-Gupta Efficiency (KGE). For that purpose, the catchment fractional snow cover area (fSCA) from the MOD10A2 dataset available at an 8 days resolution (Hall and Riggs 2016) was used as observed data. For that purpose, MOD10A2 fSCA was downloaded for the period 2000-10-15 to 2021-05-25 and aggregated at the large catchment scale. The choice of calibrating the snow parameters at the catchment scale (instead of calibrating its spatial distribution) was motivated by the fact that the Vantaanjoki catchment (which is more influenced by snow than the other catchments) is characterized by flat topography and the snow accumulation and snowmelt processes are assumed to be spatially uniform in the catchment. For the Ain, Fekete, Morava, and Krka catchments, snow cover is mainly located in the mountainous areas and has a limited impact on the hydrological response. The Guadiaro River Basin is not characterized by a regular winter snow cover, and therefore, snow calibration was neglected for Spain.

For the snow calibration, the NSGA-II algorithm (Deb et al. 2002) with 1000 iterations was used for the automatic calibration, and the KGE as an objective function. The model time series were split into a period of initialization (1995 to 2000), a period of calibration (even years from 2000 to 2020), and a period of validation (remaining years from 2000 to 2020).

2.3.2 Calibration of discharge

Measured streamflow available at different gauging stations (2 to 23 stations depending on the DRN) was used for model calibration and validation to quantify the model's ability to simulate hydrological processes in different parts of the catchment. For this purpose, the available streamflow data was split into two periods for calibration and validation (Table 2.4). These datasets as well as different statistical criteria were used for the model optimization in all 6 DRNs. In this work, several efficiency criteria were used, but only the Kling-Gupta-Efficiency was used to present the results (section 3.2) since this measure aggregates different objectives, representing the overall bias, correlation, and variability (Gupta et al. 2009). The KGE ranges from -∞ to 1, where 1 represents a perfect fit of measured and simulated streamflow. Due to different catchment characteristics, process dynamics, and data availability in the 6 DRNs, the calibration approaches were slightly different in the two groups but were jointly agreed on and led to similar results. The calibration procedures are therefore presented separately.

The list of the calibrated parameters with their calibration range is presented in Appendix A.3; Table A1 and all the final parameter values can be found in the JAMS/J2000 model datasets (section 6).

Table 2.4: *Calibration and validation periods*

Catchment	Initialization period	Calibration period	Validation period
Krka	01/10/2000 - 30/09/2002	01/10/2002 - 30/09/2012	01/10/2012 - 01/01/2020
Guadiaro	01/10/1998 - 30/09/2002	01/10/2002 - 30/09/2012	01/10/2012 - 03/07/2018
Guadiaro - Genal	01/10/1998 - 30/09/2001	01/10/2001 - 01/02/2004	30/10/2012 - 02/07/2018
Velička	01/10/1998 - 30/09/2002	01/10/2002 - 30/09/2012	01/10/2012 - 30/09/2020
Ain	01/10/1990 - 30/09/1995	01/10/1995 - 30/09/2009	01/10/2009 - 01/01/2020
Fekete	01/10/1995 - 30/09/2000	01/10/2000 - 30/09/2012	01/10/2012 - 03/07/2019
Vantaanjoki	01/10/2000 - 30/09/2005	01/10/2005 - 30/09/2014	01/10/2014 - 31/12/2020

Model calibration and validation (Guadiaro, Morava, Krka catchments)

The models' performance of simulating the measured streamflow at multiple gauging stations was evaluated using a semi-automatic calibration method, which utilizes automatic and manual calibration techniques. To assess model performance, different performance criteria were used, which focus on different evaluation criteria, such as low-flow, high flows, and bias (Kundzewicz et al. 2018; Table 2.5).

Overall, 15 global model parameters were calibrated, which showed a moderate to high sensitivity on processes related to infiltration, evapotranspiration, percolation, soil, groundwater, and runoff routing (Appendix A.3; Table A1). Besides, hydrogeological parameters influencing the recession of the water from shallow and deep groundwater aquifers were calibrated in a spatially distributed manner. The rationale behind this was to allow a good representation of groundwater processes, which are especially important in karstic regions, such as in Krka (Croatia).

For the automatic optimization, the multi-objective, non-dominated sorting genetic search algorithm NSGA-II was applied (Deb et al. 2002). Here, the three performance criteria NSE, NSE_{log} and pBias (Table 2.5) at different gauging stations were used in 5000 iterations to optimize the 15 parameters and hence, simulated streamflow for each DRN. Additionally, the process was repeated for different

spatially distributed hydrogeology parameter sets addressing the varying groundwater recession from shallow and deep groundwater aquifers. This resulted in several pareto-optimal model solutions, which still inherited strong differences of hydrological process patterns, considering, for example, the overland flow or groundwater contribution to the overall runoff.

Even though statistical measures have the advantage to objectively classify model performance and allow comparison across different models, they do not substitute visual interpretation of simulated and observed hydrographs and interpretation of process dynamics by domain experts (Legates and McCabe 1999; Moriasi et al. 2007). Therefore, the models were manually calibrated in a second step to fine-tune the results of the automated calibration procedure. The focus here was particularly on the representation of the runoff recession and groundwater contribution. Besides, due to the modeling of flow intermittence, the performance of modeling low flows was weighted higher than the model's ability to simulate high flows accurately. Further, when selecting the final parameter sets for the DRNs, sets showing higher performance at the smaller basin were given preference over sets showing higher performance at the larger basin.

During calibration, the following hydrological characteristics were taken into account:

i) runoff components (Hortonian and Hewlettian runoff, subsurface flow from soil and upper groundwater zones as well as baseflow), precipitation, actual evapotranspiration, and soil saturation;
ii) seasonal and annual water balances;
iii) spatially distributed processes at the HRU level: runoff generation, interflow, soil water balancing, evapotranspiration, and groundwater recharge.

Finally, from all pareto-optimal solutions identified through automatic and manual calibration, the most plausible model in terms of process representation according to the observed data and the knowledge about environmental characteristics was selected.

Table 2.5: Efficiency criteria used for automatic model calibration and performance evaluation (Gupta et al. 2009)

Efficiency criteria	Definition and reason for selection
Nash-Sutcliffe Efficiency (NSE)	Multi-objective function, strong focus on simulation of peak flows, widely used
Logarithmic Nash-Sutcliffe Efficiency (NSE_{log})	Like NSE, but logarithm focuses on the representation of simulation of low flows
Relative Volume Error (pBias)	Representing overall under or overestimation
Kling-Gupta-Efficiency (KGE)	multi-objective function, representing bias, correlation, and flow variability

Model calibration and validation (Ain, Fekete, Vantaanjoki catchments)

The calibration for the Ain, Fekete, and Vantaanjoki catchments also uses a multi-stations and multi-objectives approach, but using a different method. 15 global parameters related to evapotranspiration, infiltration in the soil layer, and percolation to the groundwater layer, as well as 4 spatially distributed parameters related to the groundwater reservoirs, are calibrated (Appendix A.3; Table A1). The calibration and validation periods (Table 2.4) were selected based on the availability of the observed discharge data in the different river basins.

In a first step, the Latin Hyper Cube Sampling (LHS) is used to generate 5000 model runs for each pilot river basin (the calibration ranges are provided in Appendix A.3; Table A1). Then the calibrated set of parameters is selected among the 5000 parameters sets so that the model performs best on (i) a multi-objective function (MOF) representing KGE, low-flows (10th percentile Q10), and mean annual outflow (Qyr), (ii) all the stations.

The MOF function is computed for all stations and all parameter sets (Eq. 1), then a weighted average over the stations is calculated to prioritize the stations located at the outlets of the large and small river basins ($Ref1$) and the other stations located in the small river basin ($Ref2$) (Eq. 2) (other stations located in the large catchment are referred as $Ref3$). The final calibrated set of parameters is selected among the model runs leading to the lowest $MOF_{all\ stations}$.

$$MOF = 0.6 * (1 - KGE) + 0.2 * \frac{|Q10_{sim} - Q10_{obs}|}{Q10_{obs}} + 0.2 * \frac{|Qyr_{sim} - Qyr_{obs}|}{Qyr_{obs}} \quad (1)$$

$$MOF_{all\ stations} = \frac{1}{\sum w_{Ref1} + \sum w_{Ref2} + \sum w_{Ref3}} * \left(w_{Ref1} \sum_{i \in Ref1} MOF_i + w_{Ref2} \sum_{j \in Ref2} MOF_j + w_{Ref3} \sum_{k \in Ref3} MOF_k \right)$$

with w_{Ref1} = 5, w_{Ref2} = 2, and w_{Ref3} = 1 (2)

The Ain catchment is characterized by karstic areas which have a strong impact on the hydrological response of the sub-catchments. As the JAMS/J2000 model does not represent the karst-related processes, a correction factor k was applied to the observed discharges at the gauges before comparison with simulated discharges to consider water input or water losses in sub-catchments through the karstic network (Eq. 3).

$$k = \frac{P - ET_{act} - Q}{P - ET_{act}} \quad (3)$$

with P the observed mean annual precipitation in mm (from Safran reanalysis; Vidal et al. 2010), ET_{act} the mean annual actual evapotranspiration simulated with JAMS/J2000 in mm (forced with Safran reanalysis as climate input data), and Q the observed mean annual outflow in mm.

2.4 Modeling of flow intermittence at the reach level

The results of the JAMS/J2000 hydrological models for the 6 DRNs were used to train a Machine Learning model to predict the flow intermittence at the reach level. Therefore, the Random Forest (RF) classification and regression model (Breimann 2001) was used to predict the daily state of flow (dry or flowing) at the reach level (the pool condition could not be considered in the flowing conditions due to a lack of observed data as emphasized in D1.1; Künne and Kralisch (2021). RF models have already been used to predict the perennial or intermittent flow regime of rivers at the catchment scale in González-Ferreras and Barquín (2017), and in Beaufort et al. (2019), a comparison of 4 different classification models to predict the flow intermittence showed good performances using the RF model.

The model uses 20 explanatory variables (based on Beaufort et al. (2019); Table 2.6): reach characteristics (drainage area, slope, type of LULC, type of soil, hydro-geological class), daily hydrological variables simulated with the JAMS/J2000 model at the reach scale (discharge, groundwater contribution daily at t_0 and t_{-10}), daily meteorological and hydrological variables aggregated at the catchment scale (rainfall, temperature and evapotranspiration during the 10, 20 and 30 previous days as well as soil and, groundwater saturation). The daily hydrological variables

simulated with the JAMS/J2000 model used as input data for the RF model are simulated from 2005-10-01 to 2021-09-30.

As output, the RF model gives the flow class (0=dry or 1=flow) for each tree of the random forest. For each day and each reach, if the mean of all the trees is lower than 0.5, the reach is considered dry, otherwise the reach is considered flowing.

For each DRN, the RF model was trained with 75 % of observed flow data and tested on the 25 % of the remaining data. For that purpose, the RF models were implemented and calculated using the R package "randomForest" (Liaw and Wiener 2002).

The trained RF models are then used to extrapolate the daily state of flow for every reach in the DRNs during the simulation period (2005-10-01 – 2021-09-30).

Table 2.6: *Variables of training data set for the RF model*

explanatory variables			**dependent variable**
hydrological model results for each reach	**hydro-climatological model results aggregated at the catchment scale**	**reach characteristics**	**training data**
Discharge [m3/s]	Incoming liquid water (rainfall + snow melt), sum [mm] of 10, 20, 30 days	drainage area of the specific reach [km²]	observed flow data [0=dry, 1=flowing,]
Mean discharge of 10 days [m3/s]	Air temperature, mean [°C] of 10, 20, 30 days	strahler order [-]	
Groundwater contribution to the discharge [m3/s]	Actual evapotranspiration, sum [mm] of 10, 20, 30 days	reach slope [%]	
Mean groundwater contribution to the discharge of 10 days [m3/s]	indicator of soil saturation [-] (actual volumetric soil water content / maximal volumetric soil water content [m³/m³], range 0 - 1)	hydro-geological classes	
	indicator of groundwater level [-] (actual groundwater/maximum of actual groundwater, range 0 - 1)	soil classes	
		LULC classes	

n order to evaluate the ability of the Random Forest model to represent the dry and flowing events, four efficiency criteria are computed: the probability of prediction of dry events (POD drying), the probability of prediction of flowing events (POD flowing), the false alarm ratio of dry events (FAR dry), and the false alarm ratio of flowing events (FAR flowing) (Table 2.7).

Table 2.7: Efficiency criteria for the evaluation of the RF model

		Observed	
		dry	**flowing**
Simulated	**dry**	a	b
	flowing	c	d

POD dry = a / (a+c)

POD flowing = d / (b+d)

FAR dry = b / (a+b)

FAR flowing = c / (c+d)

3 Results

3.1 Modeling entities

The processed input classes as well as the delineated Hydrological Response Units (HRUs) and reaches are shown exemplary for the Guadiaro River Basin (Appendix A.2; Figure A2.1). The overlay of the different classes delineated from the DEM (slope, aspect), LULC, soil, hydrogeology (Figure A2.1 a) - e)) resulted in 9,557 HRUs and 2,825 reaches (Figure A2.1 f)), which equals an average HRU size of about 16 ha and an average minimal drainage area for the reach of 53 ha. The delineations were done for all 6 DRNs and are summarized in Table 3.1. Besides, the discrepancies between the original river networks from the DRN teams and the computed river networks for each DRN were explained in separate documents (section 6) and is shown for the small watersheds of the 6 DRNs in Appendix A.1; Figure A1.1 – A1.6).

Table 3.1: Average area of the modeling entities for the JAMS/J2000 models and information about thresholds

River Basin	Mean HRU size [ha]	Min reach drainage area [ha]	average length of reaches [m]	Info
Guadiaro (Spain)	15.7	53.0	960	-
Fekete (Hungary)	24.1	50.0	1043	some of the artificial channels in the Fekete reference river network are not represented in the model
Ain (France)	29.2	37.5	820	resolution increased to match sampling sites
Krka (Croatia)	12.9	25.0	677	resolution increased to match sampling sites
Morava (Czech Republic)	35.7	72.0	1146	lowest resolution due to large basin area (A = 9,380 km²)
Vantaanjoki (Finland)	21.2	35.0	872	resolution increased to match sampling sites

3.2 Hydrological process dynamics at the six DRNs

In the following, results of the hydrological modeling with JAMS/J2000 are shown for each DRN separately. Plots are shown for the gauging station inside or at the outlet of the small watershed as well as closest to the outlet of the large watershed. Besides, efficiency criteria are shown for all gauges available for the DRN. The results are shown for the calibration and validation period using the KGE efficiency criteria.

3.2.1 Krka River Basin (Croatia)

The results of the hydrological modeling show a very good representation of the simulated streamflow for the small watershed Butižnica at the station Bulin Most during both model calibration and validation. The model replicates high-flows, low-flows and the water balance very well, which is shown by a KGE of 0.84 during calibration and 0.82 during validation (Figure 3.1). The model performance at the outlet of the Krka catchment Skradinski Buk replicates runoff dynamics, such as the runoff reaction to rainfall events, recession and especially low-flows very well (NSE_{log} 0.78 during calibration and 0.5 during validation). However, due to the underestimation of high-flows the bias is negative and

therefore KGE only moderate for this station. This compromise was accepted for the model's ability of simulating low-flows very accurately (Figure 3.3), and under consideration of the overall aim of modeling flow intermittence.

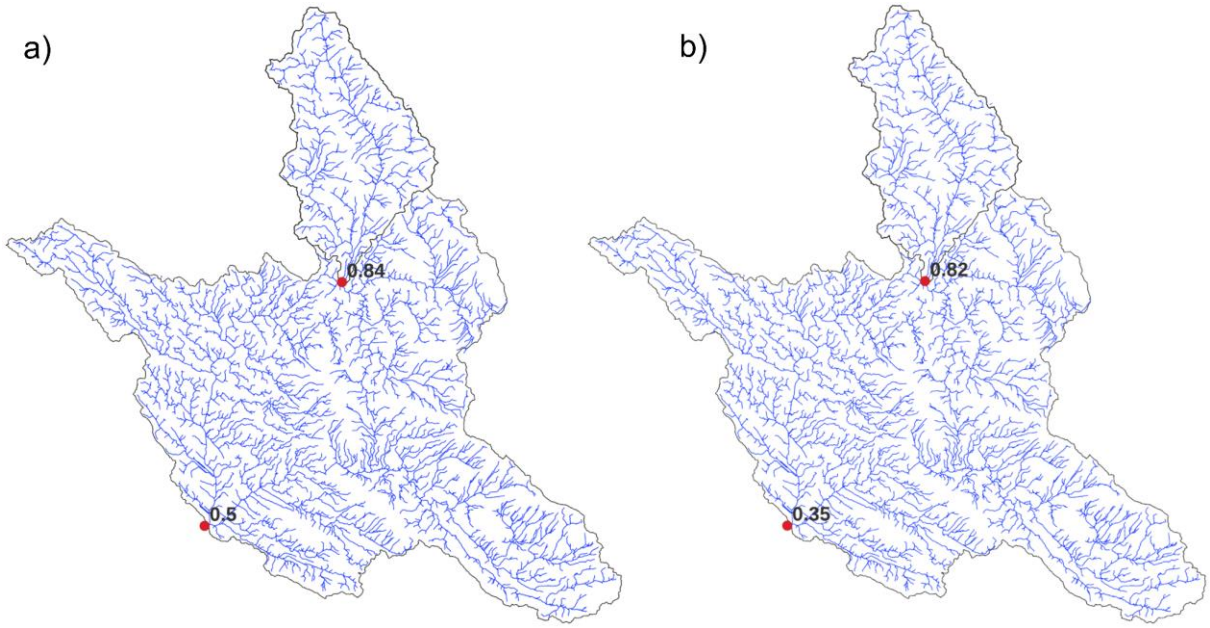

Figure 3.1: KGE for the a) calibration period (2002-2012) and b) the validation period (2012-2020) for the Krka catchment.

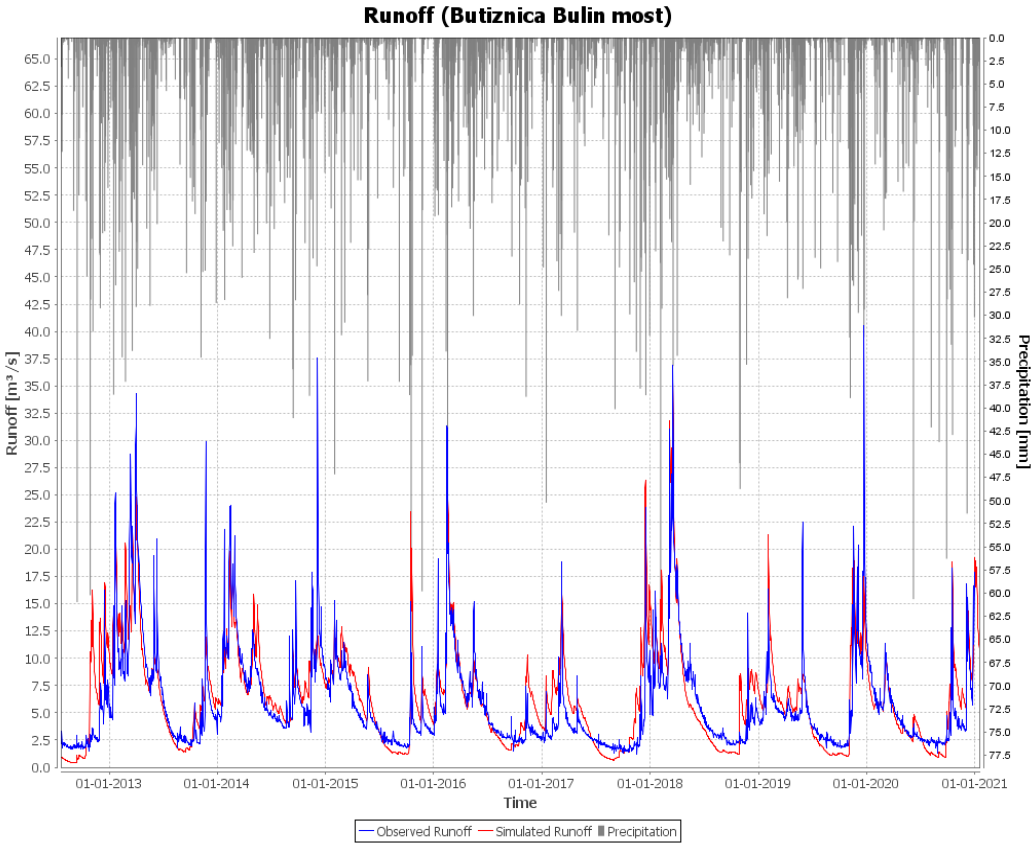

Figure 3.2: Simulated (red) and observed (blue) discharge at the Bulin most gauging station (in the Butižnica catchment). KGE calibration = 0.84, KGE validation = 0.82

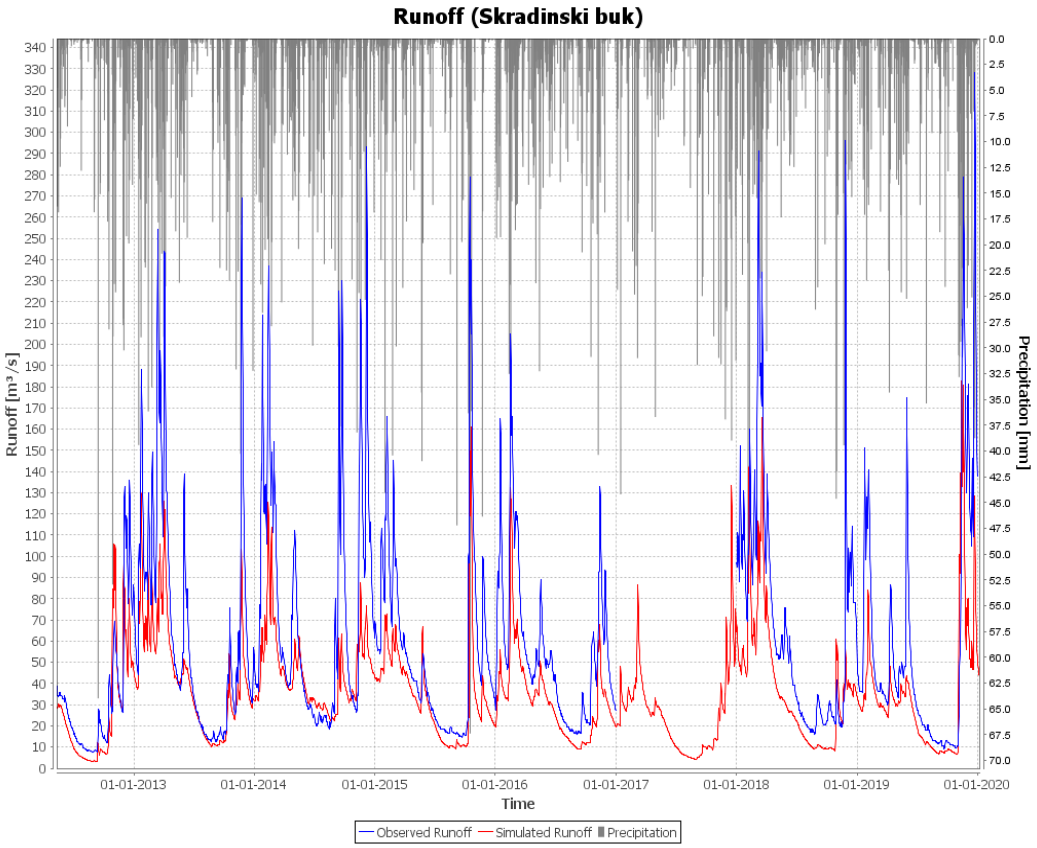

Figure 3.3: Simulated (red) and observed (blue) discharge at the Skradinski buk gauging station (in the Krka catchment). KGE calibration = 0.50, KGE validation = 0.35

3.2.2 Guadiaro River Basin (Spain)

The model performance of simulating discharge within the Guadiaro river basin shows a different picture for the different gauging stations within the basin as well as between the periods of calibration and validation, which is expressed by moderate to good KGE values (Figure 3.4). Gauging stations in Guadiaro are not located at the outlets of the small and large watershed. For that reason, the station draining the largest area (Pablo Buceite) was selected as the outlet for Guadiaro and the only station in Genal (Jubrique) used to evaluate the modeling performance in the small watershed, Genal. Additionally, an inhomogeneous pattern was found for the measured streamflow at the station Jubrique in Genal, which is why only specific years were used for calibration and validation (section 4.2.3). Besides, another station, located in the upper Guadiaro (Tr. Majaceite) was rejected completely due to inhomogeneity.

The model shows a good performance in replicating the streamflow at station Jubrique in the Genal watershed, especially predicting the summer low flows (Figure 3.5). The modeling of the discharge at the station Pablo Buceite, located in the downstream Guadiaro river shows a similarly well representation of the hydrological dynamics during high and low-flows as well as in between, during ascending and descending flow conditions (Figure 3.6). However, the station Pablo Buceite (Guadiaro) shows an over prediction during calibration and an underprediction during the validation period, which was not detected in the Genal or Hozgarganta river. The observed discharge increases during the validation period, which was not observed for the ERA5-Land precipitation data. Therefore, the reason for that could also be related to data inconsistencies, which were also observed in Jubrique (Genal) as well as Tr. Majaceite (Guadiaro upstream; section 4.2.3). For these reasons, the model was considered to work well and used for further predictions.

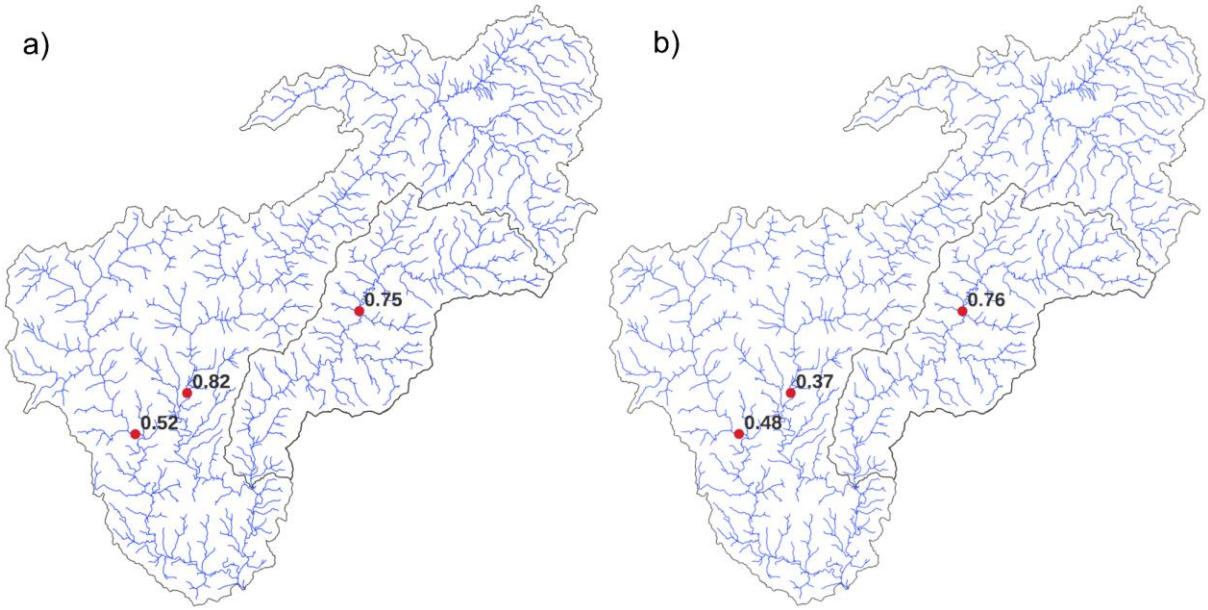

Figure 3.4: KGE for the a) calibration period (2002 - 2012; Genal: 2001 - 2004) and b) the validation period (2012 - 2018) for the Guadiaro catchment

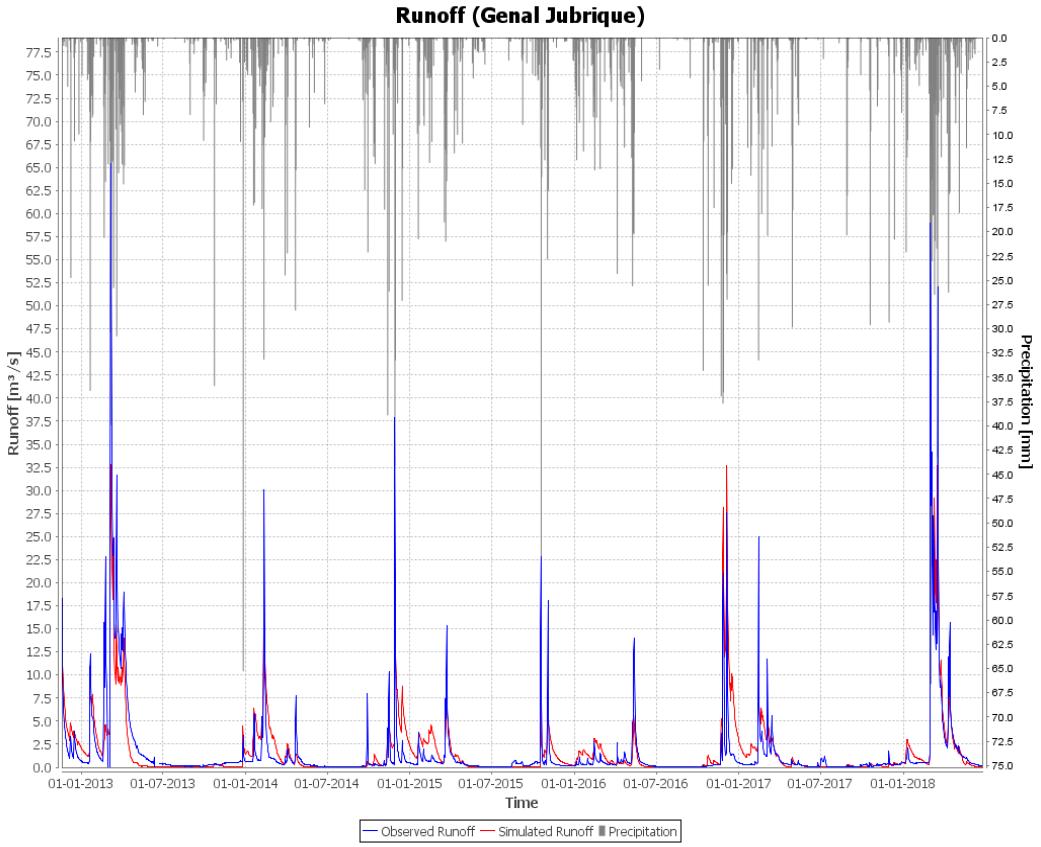

Figure 3.5: Simulated (red) and observed (blue) discharge at the Jubrique gauging station (in the Genal catchment). KGE calibration = 0.75, KGE validation = 0.76

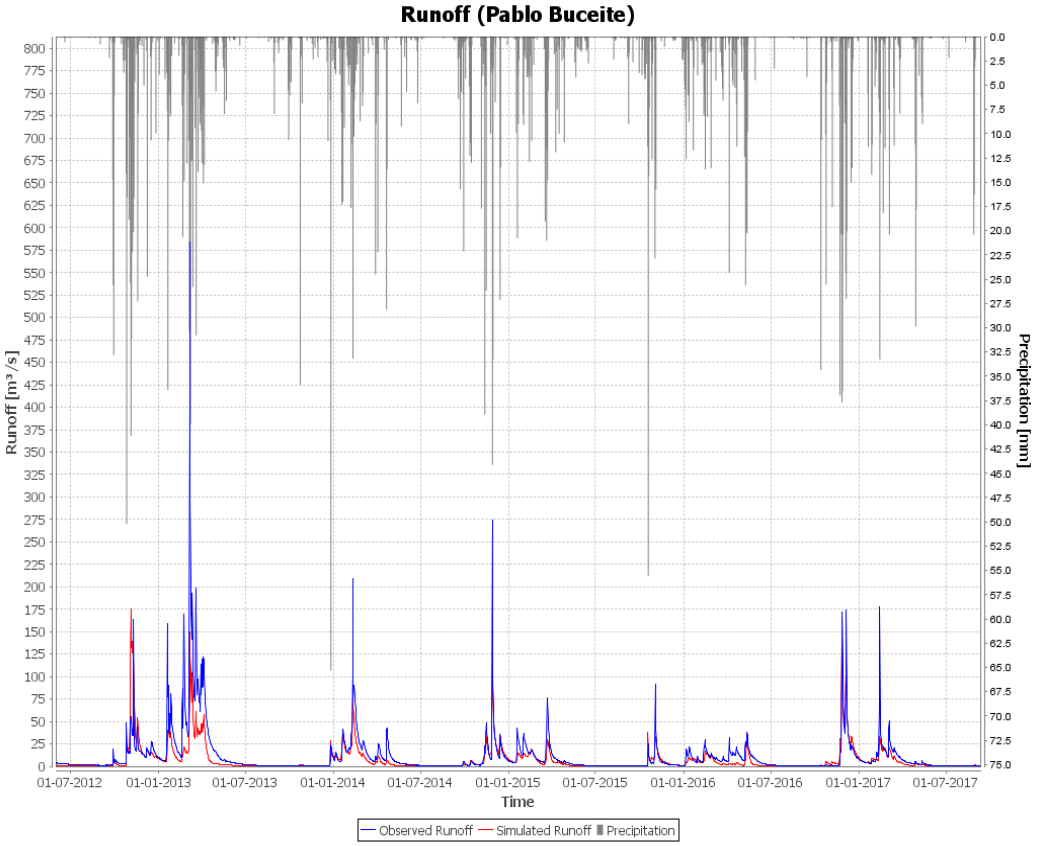

Figure 3.6: Simulated (red) and observed (blue) discharge at the gauging station Pablo Buceite (in the Guadiaro catchment). KGE calibration = 0.82, KGE validation = 0.37

3.2.3 Morava River Basin (Czech Republic)

The results of the hydrological modeling in the Morava River Basin show a good representation of the observed discharge throughout the basin with satisfactory to good KGE values, ranging from 0.49 to 0.82 during the calibration period, and from 0.37 to 0.73 during the validation period. The model performance shows good results in simulating the streamflow dynamics measured at the 7 stations along the Morava river, manifesting in KGE values ≥ 0.6 during the validation period (Figure 3.7). Whereas the model performance for the smaller Velička catchment shows a satisfactory, but worse replication of streamflow dynamics than in the large catchment. The model overpredicts discharge in certain years, such as 2015 (Figure 3.8). It is however, important to mention that the year 2015 was overpredicted at most stations and also at the outlet station of the large catchment, Morava Strážnice (Figure 3.9). This phenomenon could not be observed in other years at the stations in the main stem of the Morava river.

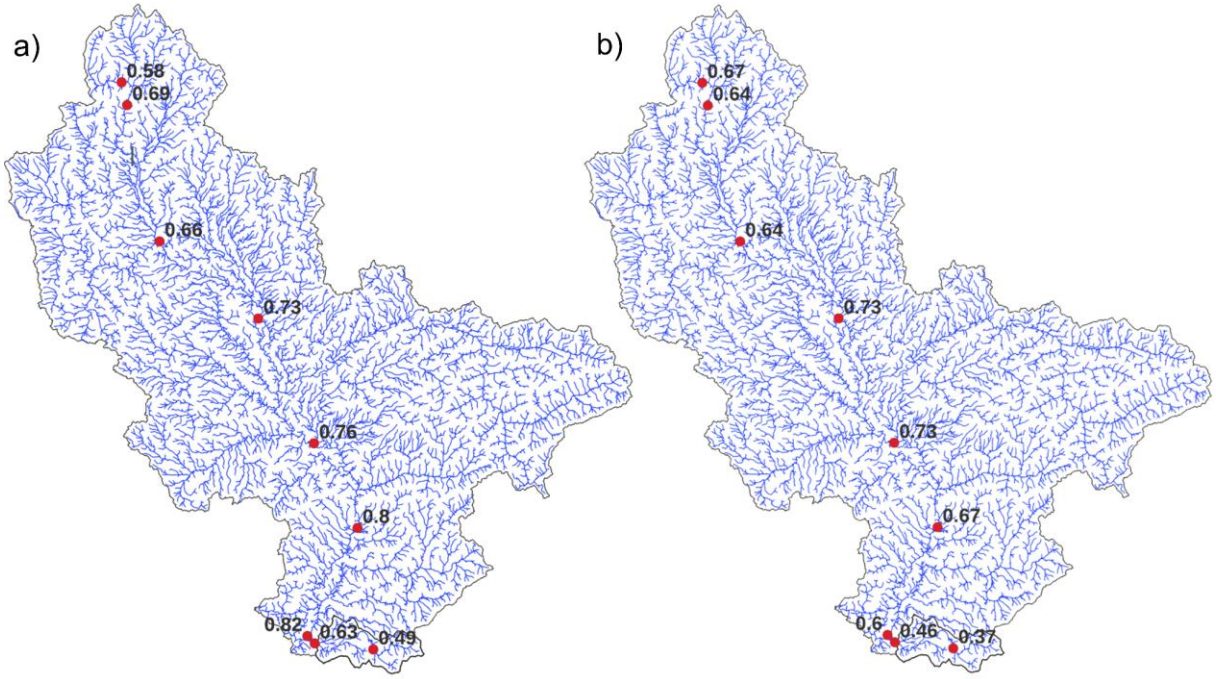

Figure 3.7: KGE for the a) calibration period (2002-2012) and b) the validation period (2012-2020; Strážnice Morava 2012-2018) for the Morava catchment

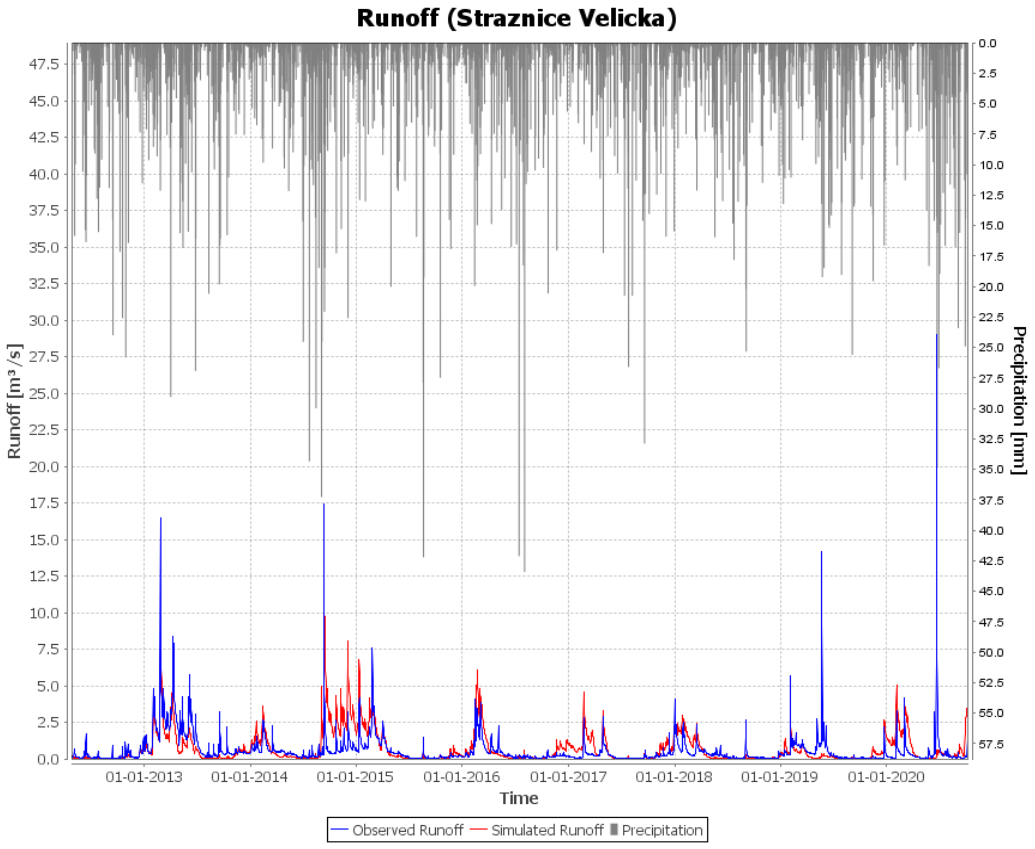

Figure 3.8: Simulated (red) and observed (blue) discharge at the Strážnice Velička gauging station (outlet of the Velička catchment). KGE calibration = 0.63, KGE validation = 0.46

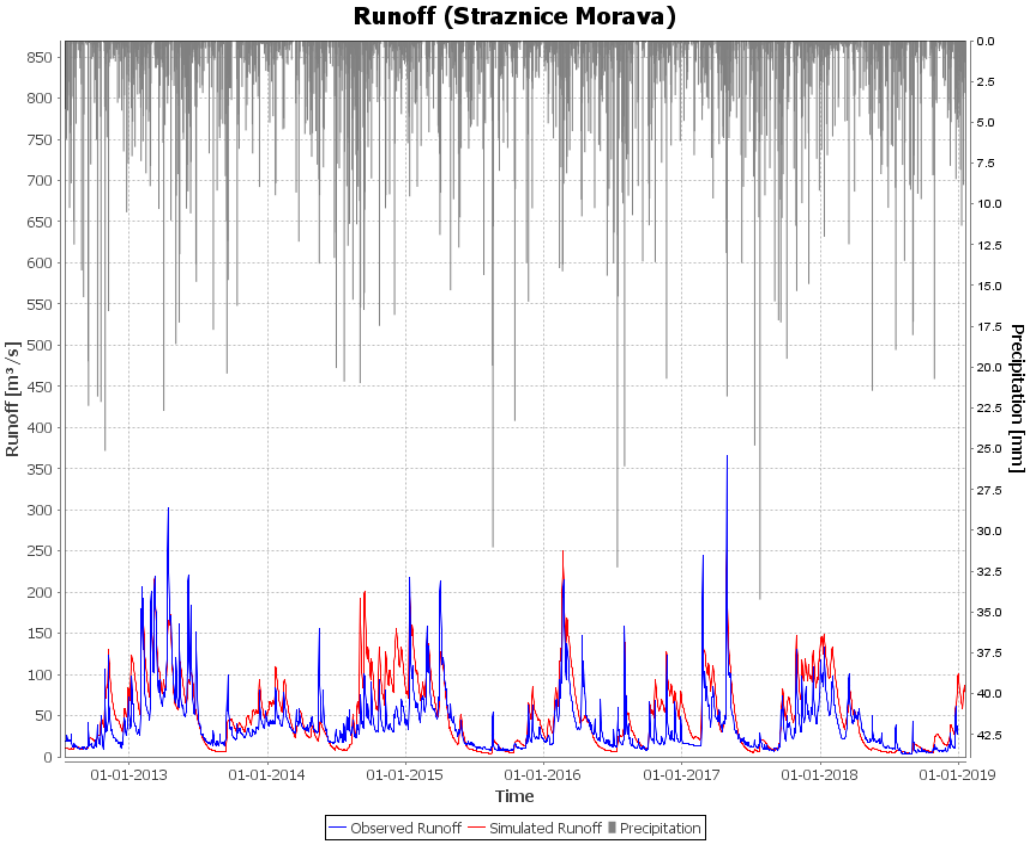

Figure 3.9: Simulated (red) and observed (blue) discharge at the Strážnice Morava gauging station (outlet of the Morava catchment). KGE calibration = 0.82, KGE validation = 0.60

3.2.4 Ain River Basin (France)

The results show a good fit between simulated and observed discharge for the Ain catchment where KGE values are above 0.6 for most of the gauging stations both during the calibration and validation periods (Figure 3.10). Figure 3.11 and Figure 3.12 show that the temporal dynamics of the discharge at the outlet of the large and small catchments are well represented by the model.

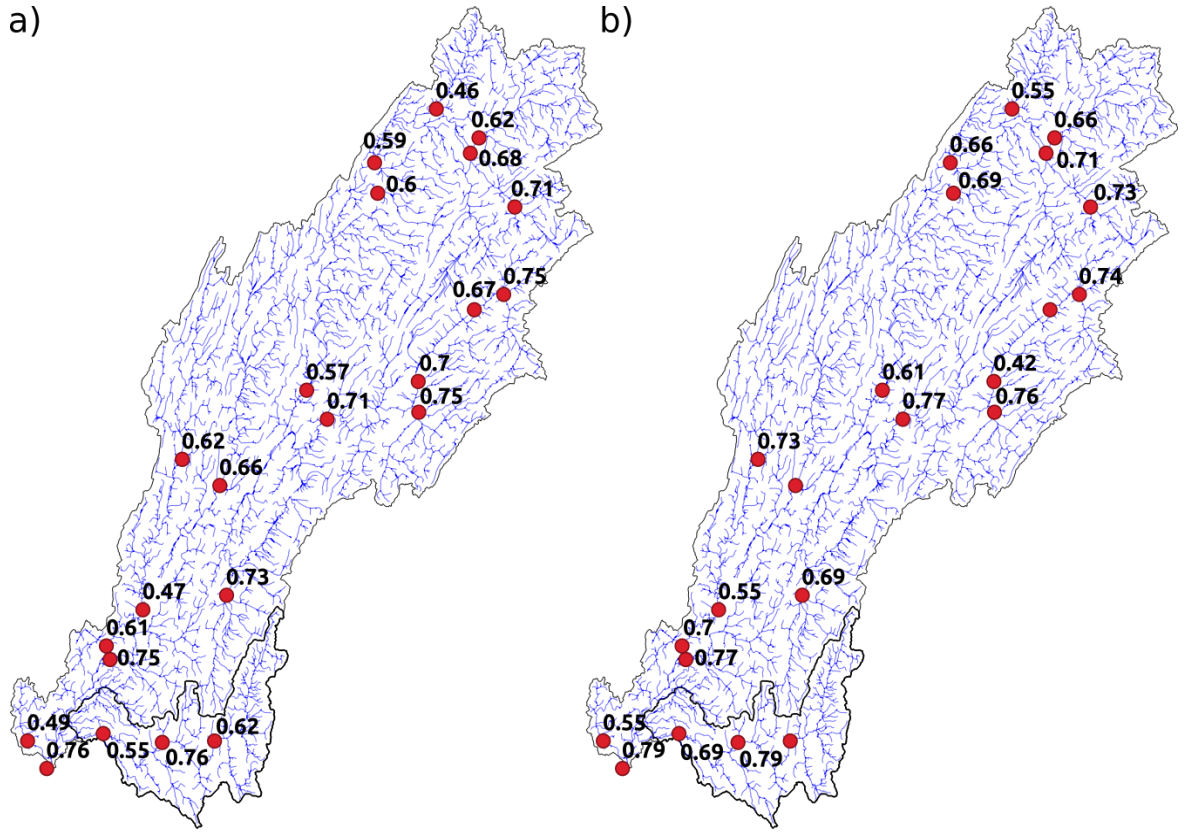

Figure 3.10: KGE for the a) calibration period (1995-2009) and b) the validation period (2009-2019) for the Ain catchment. Missing values during the validation period are due to the shutdown of gauging stations

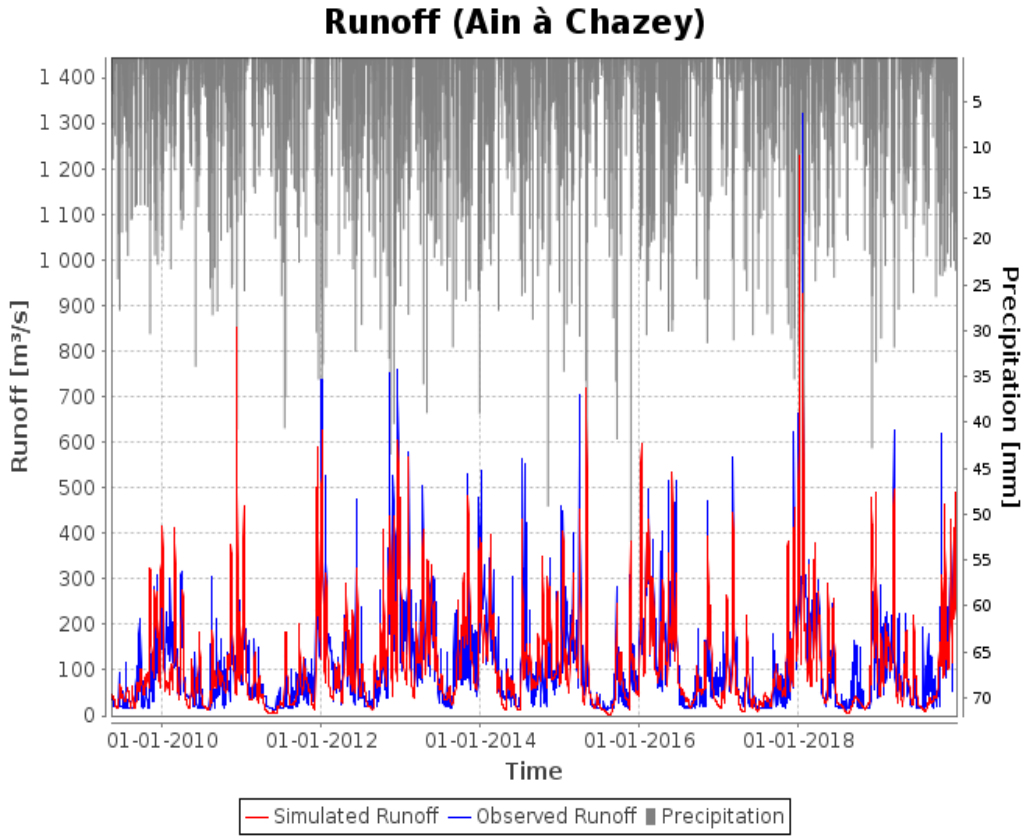

Figure 3.11: Simulated (red) and observed (blue) discharge at the Chazey station (outlet of the Ain catchment) for the validation period. KGE calibration = 0.76, KGE validation = 0.79

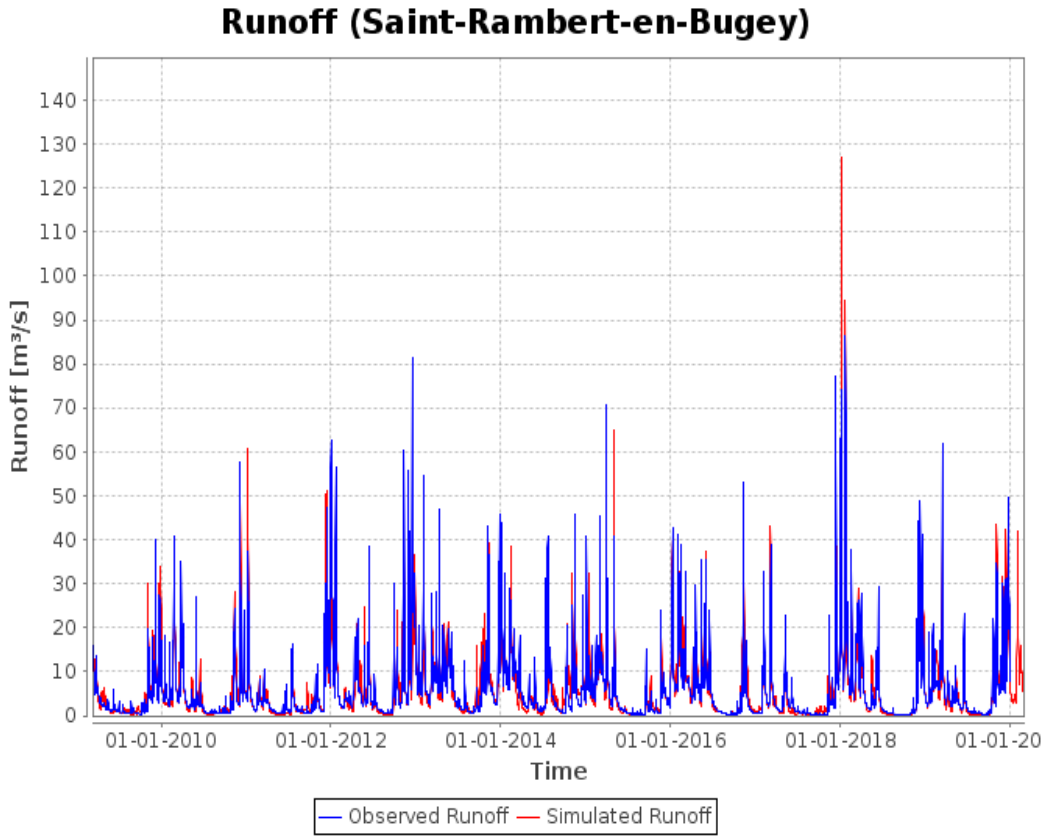

Figure 3.12: Simulated (red) and observed (blue) discharge at the Saint-Rambert station (in the Albarine catchment) for the validation period. KGE calibration = 0.76, KGE validation = 0.79

3.2.5 Fekete River Basin (Hungary)

The JAMS/J2000 shows contrasted performance in Fekete (large catchment) and Bukkosdi (small catchment; Figure 3.13). Discharges are well simulated in the Bukkosdi catchment (Figure 3.13.b and Figure 3.15), except for one station with a negative KGE during the calibration period. The differences of performances between the gauging stations in the Bukkosdi catchment may be due to the karstic area in the upstream part of the basin.

The Fekete catchment is characterized by an artificialized river network with artificial channels that could not be represented in the model which could explain the poor performance of the model in the larger catchment (Figure 3.14).

Moreover, there is an uncertainty regarding the climate input data as there is no local meteorological station in the catchment to validate precipitation and air temperature from the ERA5-land reanalysis.

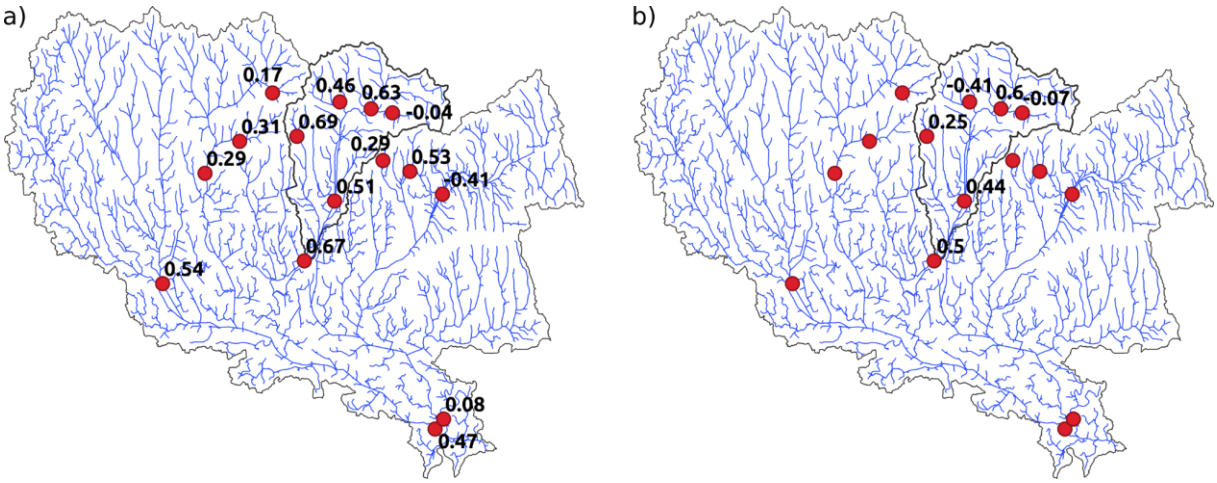

Figure 3.13: KGE for the a) calibration period (2000-2012) and b) the validation period (2012-2019) for the Fekete catchment

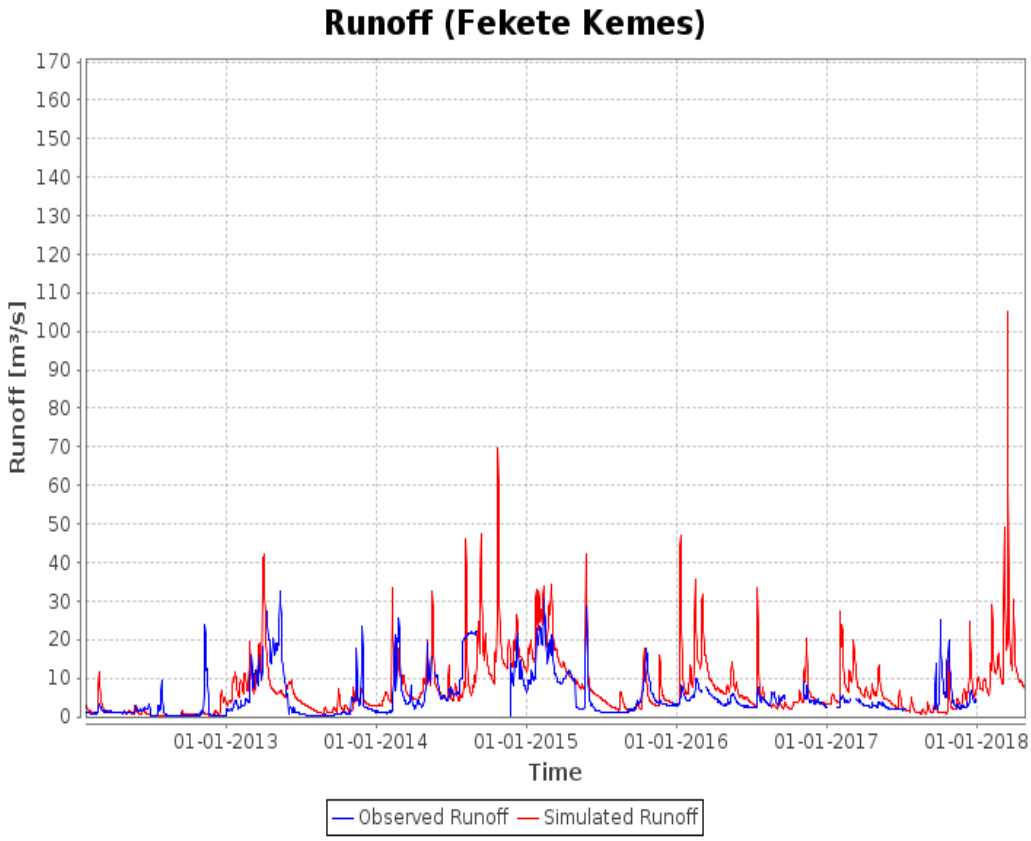

Figure 3.14: Simulated (red) and observed (blue) discharge at theKemes station (in the Fekete catchment) for the validation period. KGE calibration = 0.47

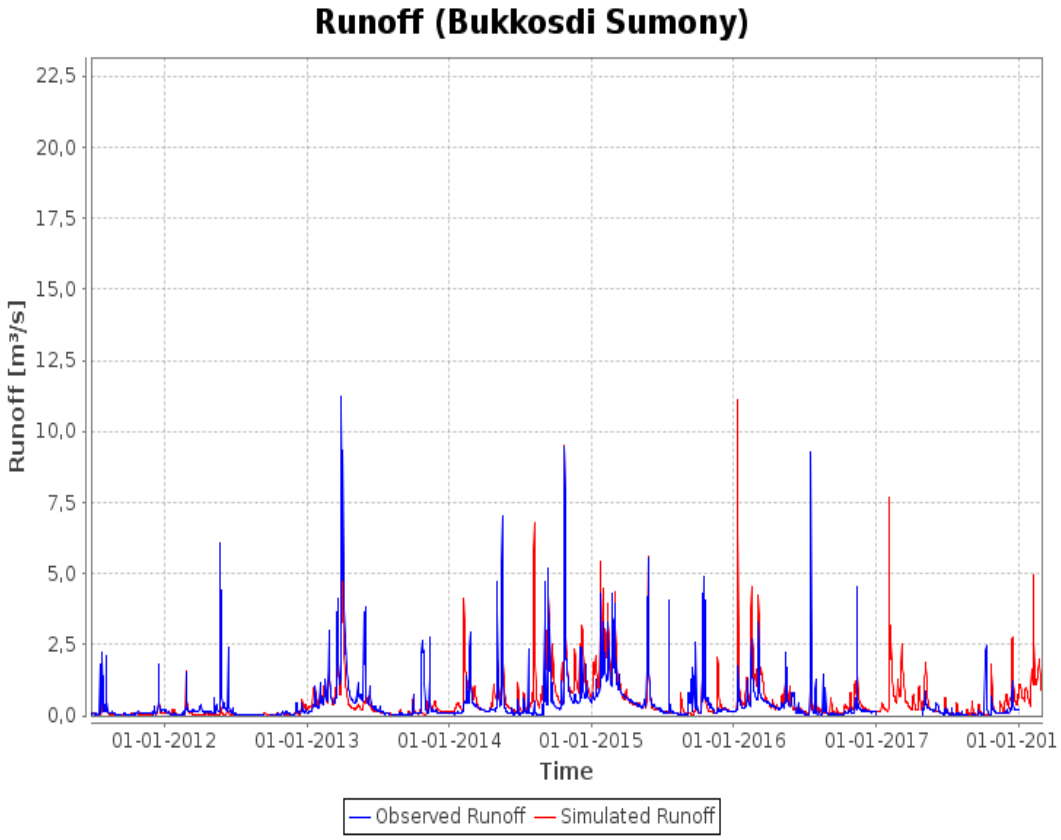

Figure 3.15: Simulated (red) and observed (blue) discharge at the Sumony station (outlet of the Bukkosdi catchment) for the validation period. KGE calibration = 0.67, KGE validation = 0.5

3.2.6 Vantaanjoki River Basin (Finland)

Discharges are overall well simulated in the Vantaanjoki and Lepsämänjoki catchments (Figure 3.16). The temporal dynamics are well represented by the JAMS/J2000 model in the Lepsämänjoki catchment (Figure 3.18), however, low-flows tend to be overestimated at the Olunkyla station (outlet of the larger catchment, Figure 3.17).

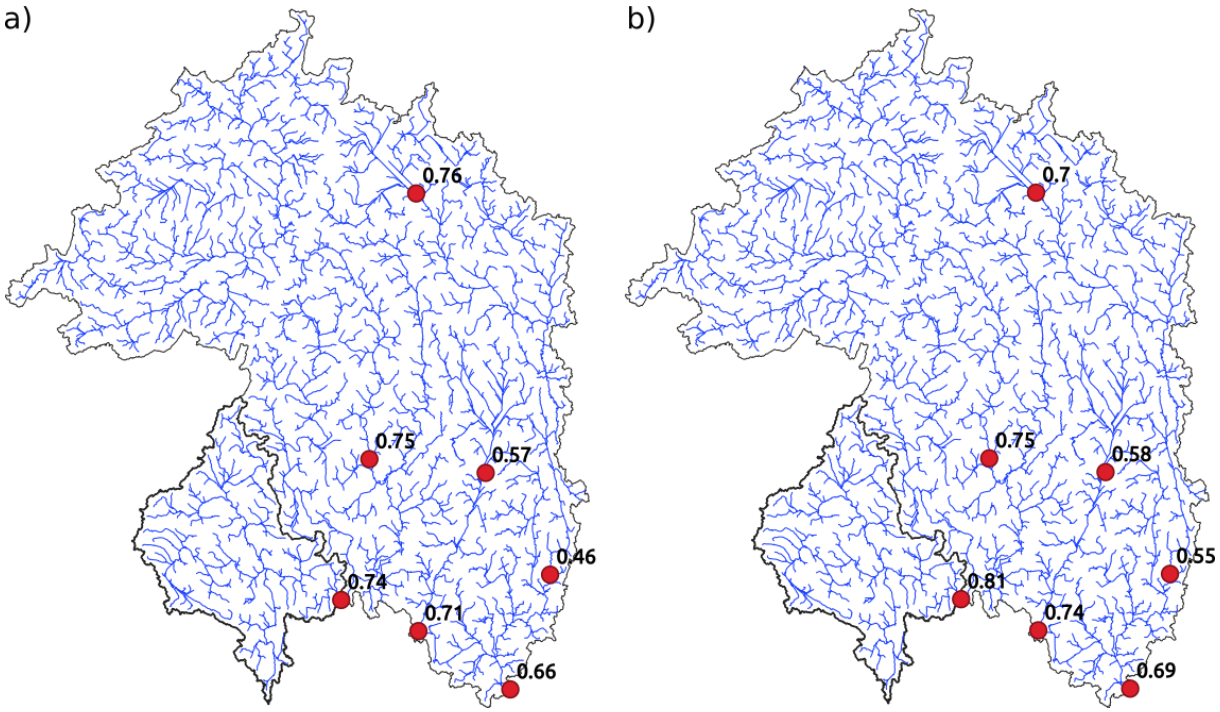

Figure 3.16: KGE for the a) calibration period (2005-2014) and b) the validation period (2014-2020) for the Vantaanjoki catchment

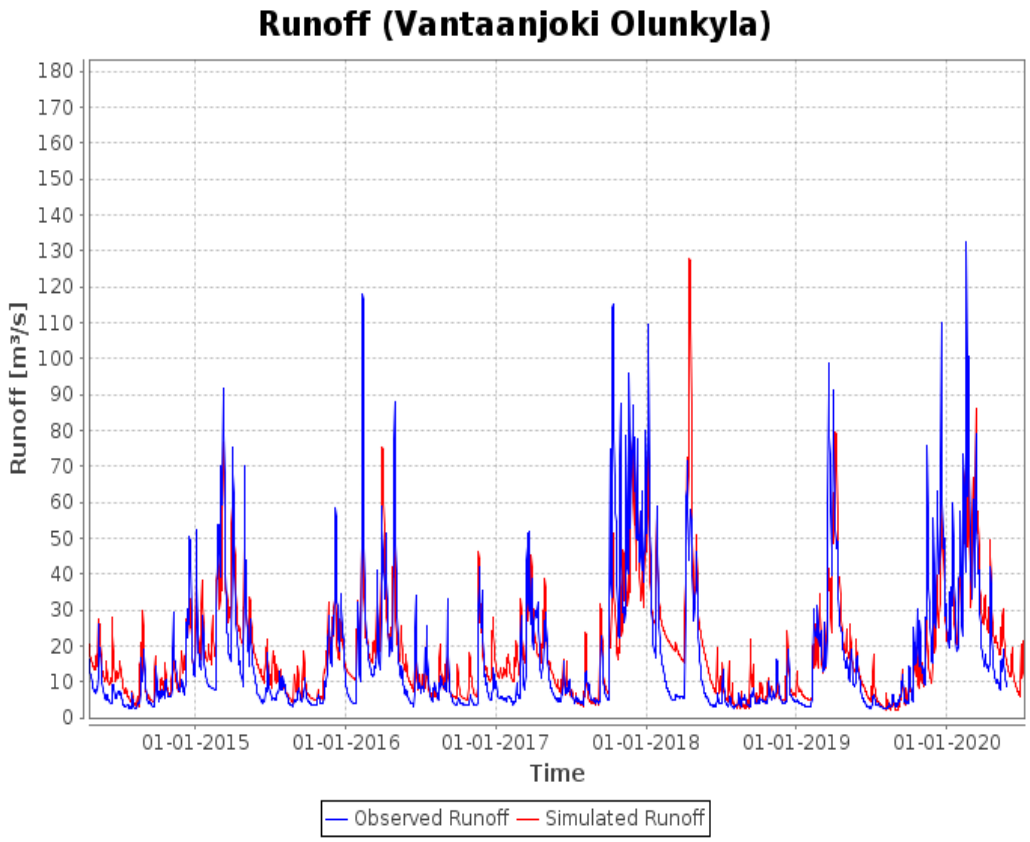

Figure 3.17: Simulated (red) and observed (blue) discharge at the Olunkyla station (outlet of the Vantaanjoki catchment) for the validation period. KGE calibration = 0.66, KGE validation = 0.69

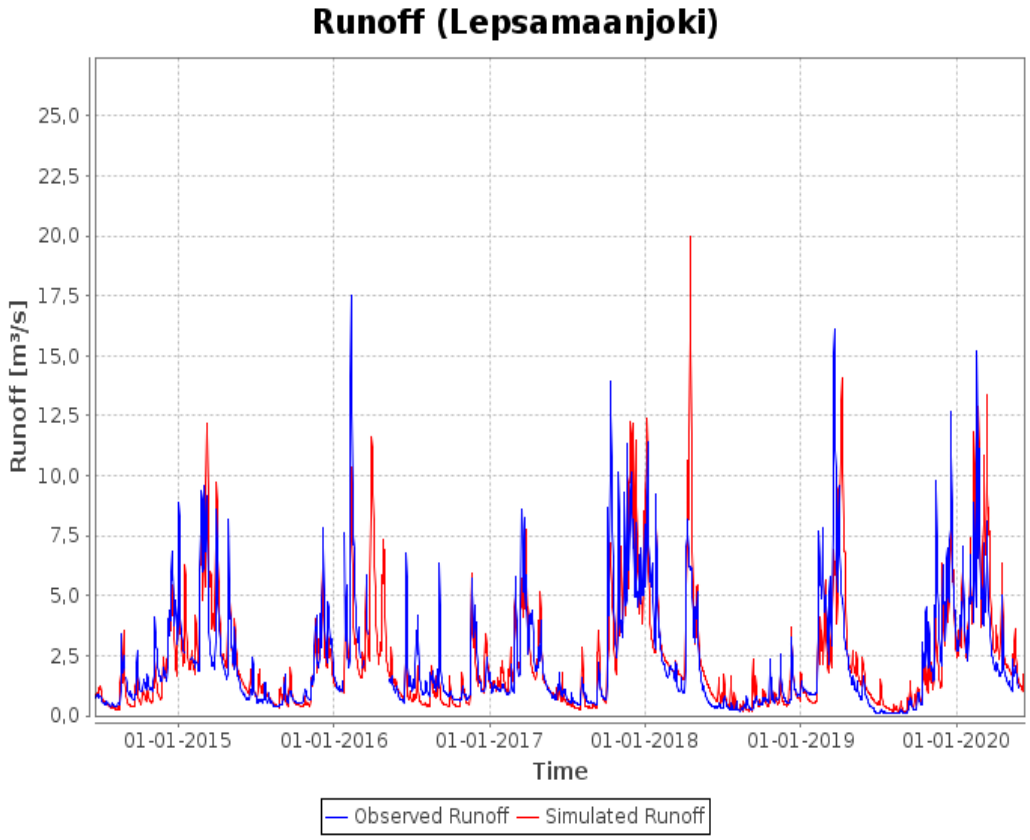

Figure 3.18: Simulated (red) and observed (blue) discharge at the Lepsämänjoki station for the validation period. KGE calibration = 0.74, KGE validation = 0.81

3.2.7 Simulation of the snow cover

The novel approach of calibrating the snow accumulation, metamorphosis and snow melt resulted in a precise replication of the snow cover area and timing in comparison to the MODIS10A2 dataset (Figure 3.19). The results for all DRNs are shown in Table 3.2, whereas the corresponding Figures are shown in Appendix A.4.

Results show very good performances for the Ain and Vantaanjoki catchments, which are the two catchments most impacted by snow. For all catchments the models are able to represent accurately the timing of the snowfalls and the duration of the snow cover.

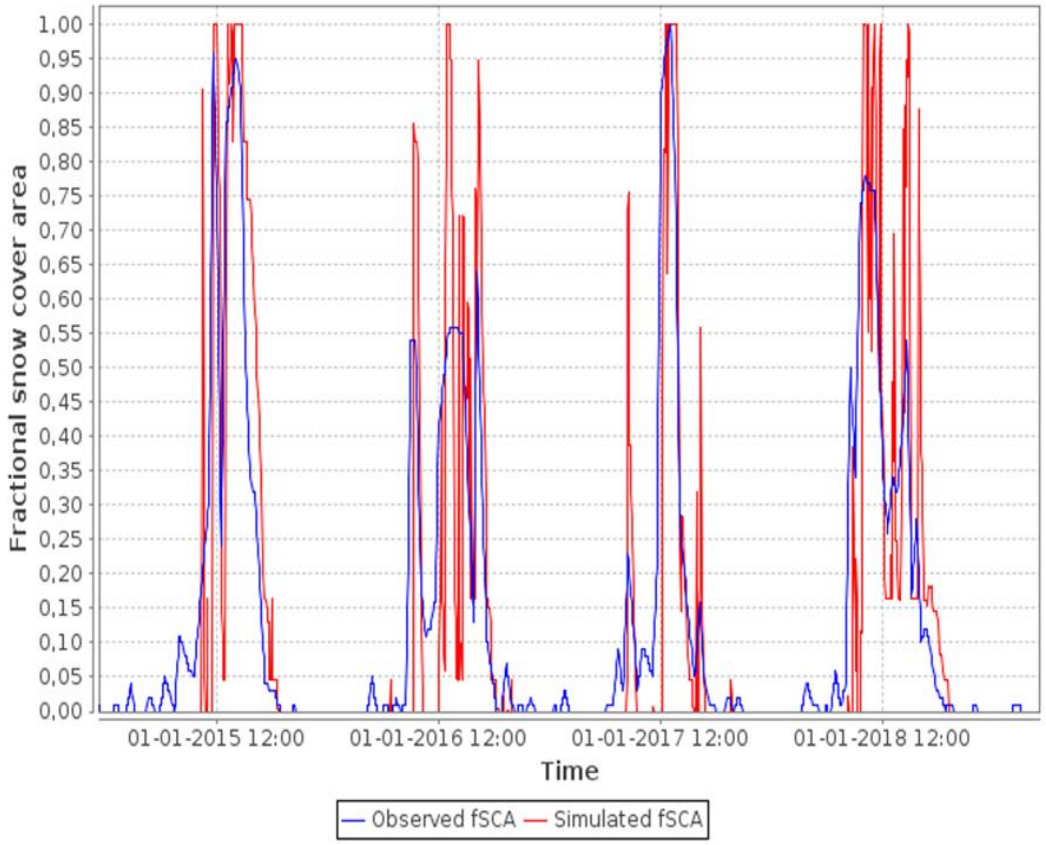

Figure 3.19: Simulated (red) and observed (blue) snow cover area (fSCA) for the Ain catchment

Table 3.2: *KGE values for the fractional snow cover area (fSCA)*

DRN	KGE calibration	KGE validation
Ain	0.81	0.74
Fekete	0.68	0.57
Krka	0.36	0.46
Morava	0.86	0.83
Vantaanjoki	0.80	0.74

3.3 Prediction of Flow Intermittence

This section presents the results for the modeling of flow intermittence for the Albarine, Bukkosdi, Genal, Lepsämänjoki, and Velička DRNs.

No results are presented for the Butižnica DRN (Croatia) due to insufficient flow intermittence data to train and validate the RF model. Available data for the Butižnica DRN are the observed discharges from the Bulin Most gauging station which is characterized by a perennial flow (Figure 3.2), and 21 observations from the DryRivers App made on the 2021-10-11 and 2021-11-11 (after the end of the JAMS/J2000 simulation period) and mostly along the main river (Table 2.3 and Figure 2.3). These 21 observations are not sufficient to characterize the temporal and spatial variability of drying in the Butižnica DRN.

Table 3.3 shows the efficiency criteria of the RF model for each DRN. The results show very good performances of the RF model in the Albarine, Bukkosdi, Lepsämänjoki and Velička DRNs with POD

drying above 90%. The RF models in the Albarine and Bukkosdi DRNs tend to slightly overestimate drying events with FAR drying above 5%.

For the Genal DRN, the POD drying and FAR drying show that the RF models do not represent dry events as well as in other DRNs. Regarding the Genal DRN, this is mainly due to the lack of available observed data used to train the RF model.

Table 3.3: *Performance of the RF model (validation dataset)*

DRN	POD dry [%]	FAR dry [%]	POD flowing [%]	FAR flowing [%]
Albarine	90.7	5	98.9	2.2
Bukkosdi	91.7	8.1	96.9	3.2
Genal	50	22.2	99.8	0.8
Lepsämänjoki	91.7	1.8	99.9	0.4
Velička	92.9	4.3	99.3	1.2

3.4 Flow intermittence indicators

The predicted flow state can then be used to compute intermittence indicators for each DRN.

Figure 3.20and Figure 3.24 present maps of the ConD intermittence indicator (mean annual number of days with a dry condition; Künne and Kralisch 2021) for the small catchments. The maps of ConD indicators allowed us to evaluate the spatial patterns of drying in the DRNs. For all watersheds, the simulated spatial patterns seem to be consistent with observations, with more drying on the smaller tributaries and less or no drying in the main river sections. These results are also consistent with observed data, showing a North-South gradient of flow intermittence from Finland to Spain: the model simulates a pronounced drying of river reaches in the Genal catchment (around 2 to 3 months of dry states in the small tributaries) and almost no drying in the major part of the Lepsämänjoki DRN, except for the smallest tributaries.

For the Albarine and Bukkosdi DRNs, Figure 3.20.b and Figure 3.21.b show a classification of the reaches based on observations provided by the DRN field teams. The comparison between the simulated and observed spatial pattern of drying shows that even if drying events seem to be overestimated along the middle of the Albarine river, the areas with observed flow intermittence in the upstream and downstream parts of the catchment are well represented by the model. In the Bukkosdi DRN, the general spatial pattern of flow intermittence is also well represented by the model. However, in the upstream part of the DRN, some reaches classified as perennial by the DRN leader/field team are simulated as intermittent. For the Genal RB the comparison of the model results and the observed data, provided by the DRN field teams (Figure 3.22.a and 3.22.b) shows a high conformity. However, the model can be improved during the next month with more data observations. Figure 3.24.a and Figure 3.24.b show the results of the RF model and the observed classifications by the DRN field teams for the Velička DRN. The calculated mean annual number of days with a dry

condition (ConD) shows a strong alignment with the observed flow conditions, especially in the downstream part of the Velička catchment.

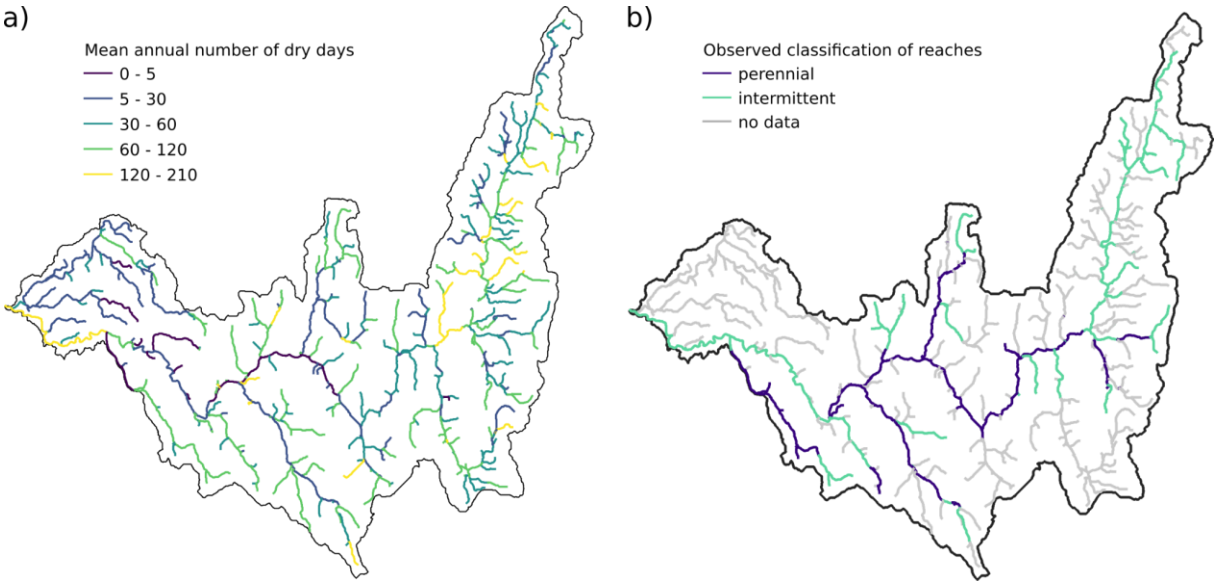

Figure 3.20: a) Maps of ConD index (Mean annual number of days with a dry condition) for the Albarine DRN, b) classification of the reaches (perennial or intermittent) provided by the DRN leader based on observations

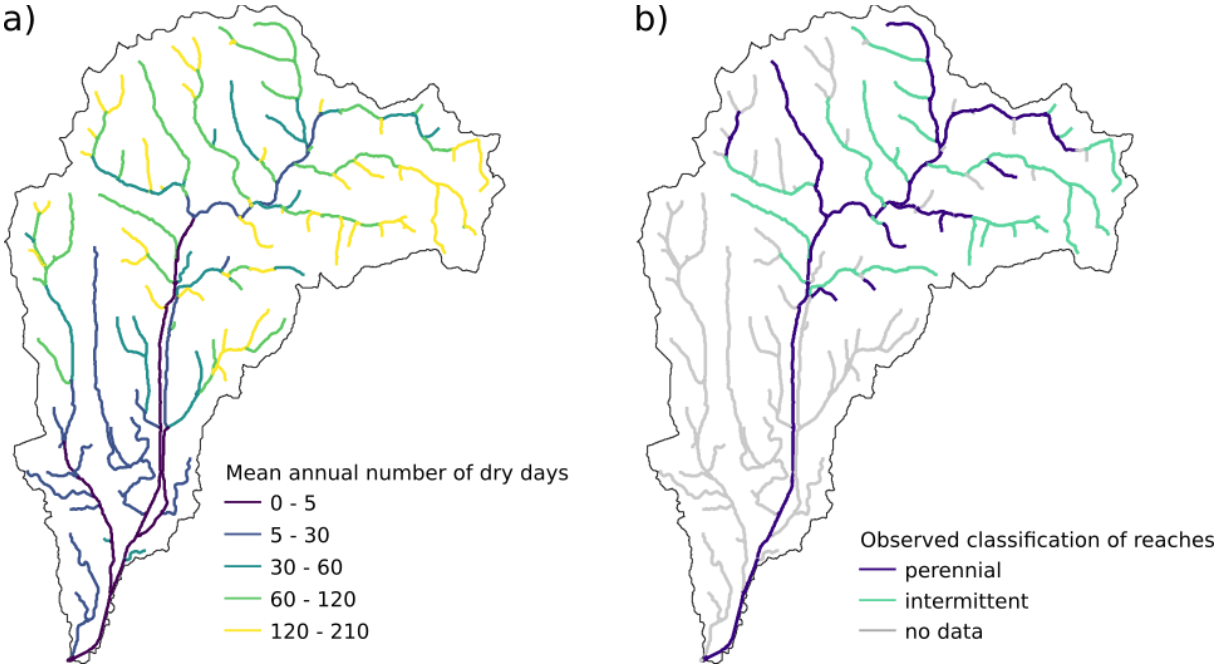

Figure 3.21: a) Map of ConD index (Mean annual number of days with a dry condition) for the Bukkosdi DRN, b) classification of the reaches (perennial or intermittent) provided by the DRN leader based on observations

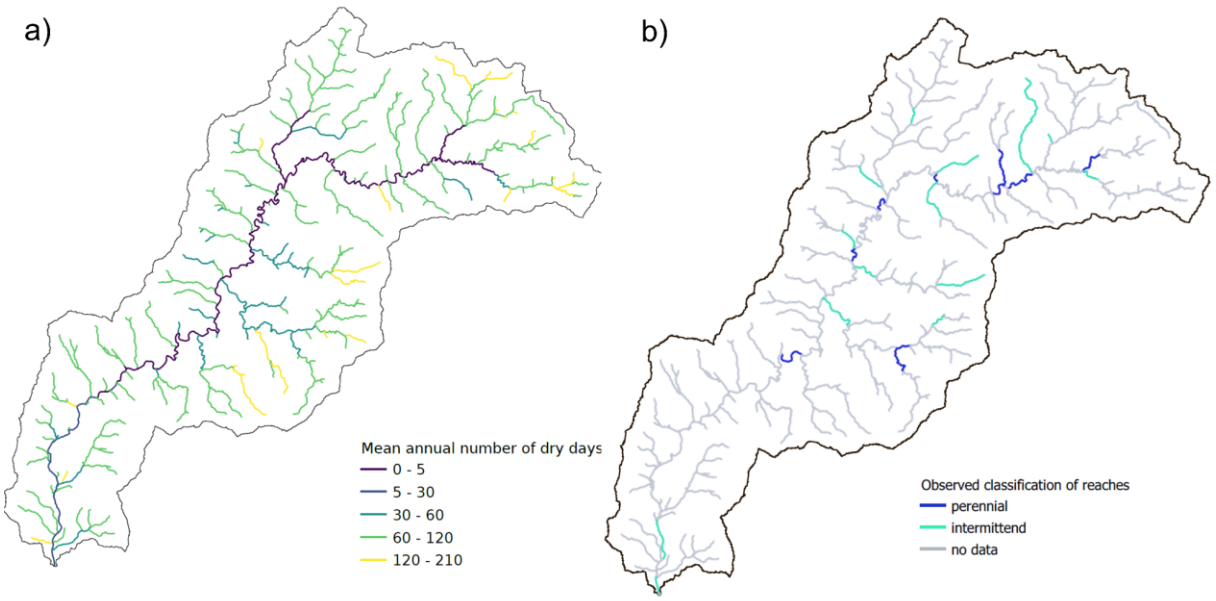

Figure 3.22: a) Map of ConD index (Mean annual number of days with a dry condition) for the Genal DRN. b) classification of the reaches (perennial or intermittent) provided by the DRN leader based on observations

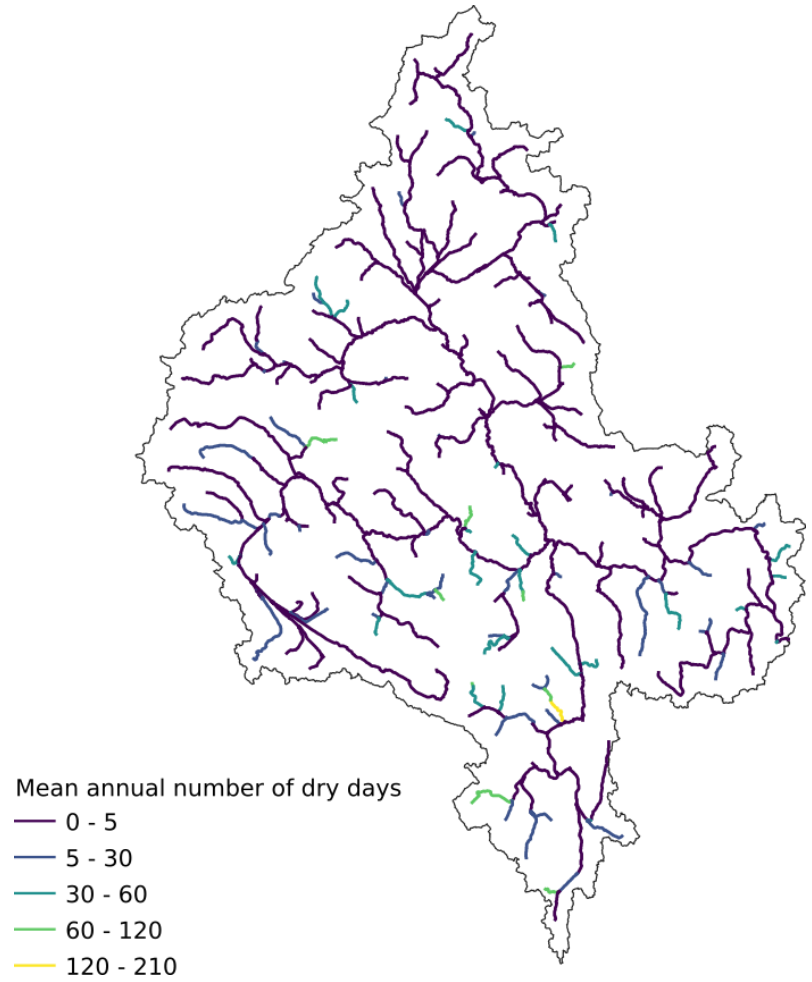

Figure 3.23: Map of ConD index (Mean annual number of days with a dry condition) for the Lepsämänjoki DRN.

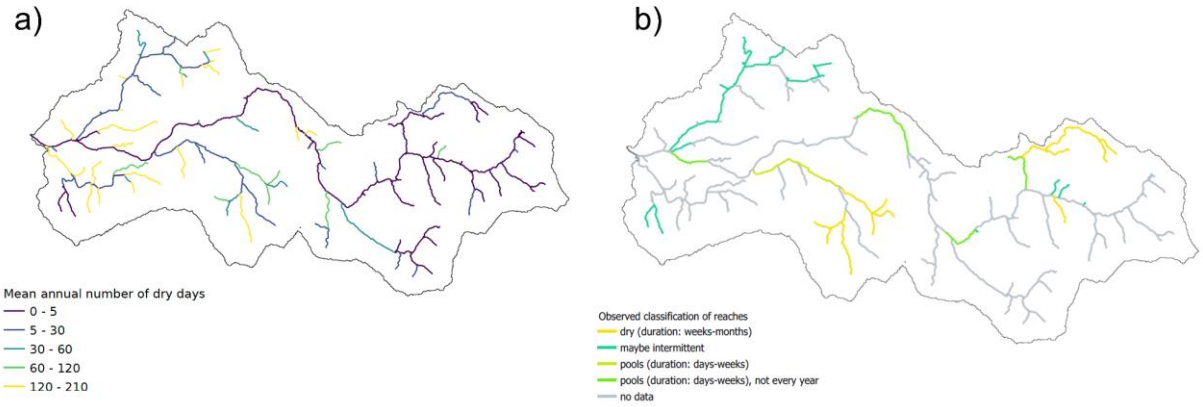

Figure 3.24: a) Map of ConD index (Mean annual number of days with a dry condition) for the Velička DRN. b) classification of the reaches (perennial or intermittent) provided by the DRN leader based on observations

4 Discussion

In this report, the discussion should address the limitations and uncertainties of both data and developed models concerning the specific tasks. Besides, an effort is made to quantify possible impacts on the objectives of DRYvER.

4.1 Generation of river networks as part of modeling entities

The generation of the river networks is part of the modeling process and incorporated into the delineation of the modeling entities, which are Hydrological Response Units (HRUs) and reaches (Section 3.1). Therefore, the synthetic river networks are mainly dependent on the DEMs, but also tightly coupled with other spatial data sets. In that process, the DEM resolution as well as the minimal drainage area selected as a threshold delimits the resolution of the river network. To assure a similar spatial basis and resolution throughout the 6 European DRNs, a minimum drainage area was chosen at the beginning of the project, which was about 30 ha to 50 ha. However, adaptations to the data were made to match the reference networks provided by the DRN leaders as well as the river networks generated by other WPs (section 6). Even though the provided river networks could not always be replicated by the available DEMs, the aim was to match the sampling points provided by WP2. This was possible in all cases, except for one sampling point in Butižnica (Croatia; BUT 08). To match this point, the minimum drainage area would have been reduced, which would result in a very high resolution and challenges in the modeling process as well as in the overall approach of using a similar resolution throughout all DRNs. Besides, the Croatian river network already has the highest resolution, with a minimum drainage area of 25ha.

4.2 Input data sets for hydrological modeling with JAMS/J2000

4.2.1 Meteorological data

Meteorological data sets are crucial to force the hydrological models. Due to inefficiencies in available locally observed data as well as the constraint of having up-to-date datasets, Mimeau et al. (2022) evaluated and compared different climate data sets to measured station data and their impact on simulated runoff of both, modeled and reanalysis products. The ERA5 Land product showed the was selected as a result of this assessment. However, the uncertainty of ERA5 Land compared to the

observed data varies a lot throughout the 6 DRNs, with considerable variability on simulated river runoff (Figure 4.1).

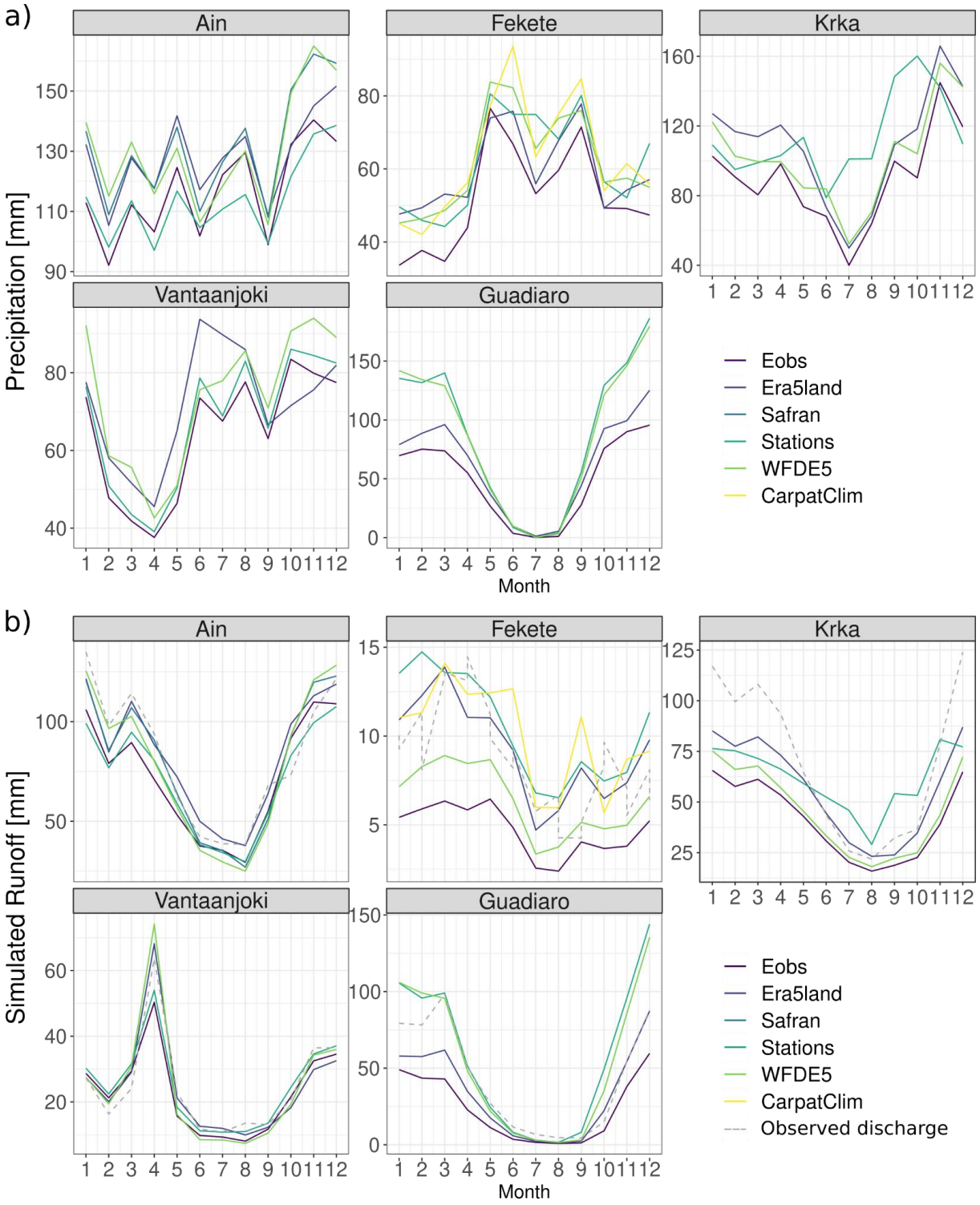

Figure 4.1: Mean monthly precipitation (a) and simulated runoff (b) in the Ain, Fekete, Krka, Vantaanjoki, and Guadiaro catchments obtained with different climate datasets: Eobs daily gridded observational dataset (Cornes et al. 2018), *Era5-land reanalysis* (Muñoz-Sabater et al. 2021), *Safran French reanalysis* (Vidal et al. 2010), *local meteorological stations* (GSOD *and https://en.ilmatieteenlaitos.fi/download-observations), WFDE5 (bias-adjusted ERA5 reanalysis;* Cucchi et al. (2020), *and Carpatclim (reanalysis on the Carpathian region;* Szalai et al. (2013)

4.2.2 Spatial data and biophysical information

European datasets were used to generate these input classes as well as calculate the model parameters, which differ in each DRN.

The analysis of the hydrogeological data (BGR 2013; Andreas and Duscher 2019) showed that Guadiaro, Fekete, Ain, and Krka share karstified rocks in some areas of the catchment. Almost 60 % of the Krka DRN and 94 % of the Ain DRN contain carbonate rocks, such as dolomite and limestone, which are often karstified (Appendix A.5; Figure A9). Karst contains different types of porosity, which complicate the modeling of these areas (Hartmann 2013). The J2000 model used in this study showed its usefulness and advantages over other models in modeling karstified systems and seepage from the alluvial river bed in the past (Fink et al. 2007; Watson et al. 2021). However, there was no data for these DRNs available to calibrate or validate the hydrogeological process dynamics in these areas.

Further, the European soil database (European Commission; Panagos et al. (2012), allowed using consistent soil classes and physical data. However, the data source is very coarse-grained and did not provide certain physical information, such as bulk density. Besides, layered information was very coarse, which only allowed a lumped modeling of soil water processes. Therefore, a local soil database with physical information of soil horizons was used for Spain (Llorente et al. 2018) to calculate physical properties with pedotransfer functions (Ad-hoc-AG Boden 2005; FAO 2006), which was a similar, but different approach than for the other DRNs. In the future, high-resolution and layered soil data could improve the models.

4.2.3 Observed river runoff

Two stations were excluded completely due to strong data inhomogeneity. These were the station Kljuice in Croatia and Tr. Majaceite in the upstream part of the Guadiaro DRN in Spain. Besides, the observed river runoff at station Jubrique in Genal showed strong inconsistencies, too (Figure 4.2). Besides, similar problems occur in discharge data from Hungary and Finland. In Hungary, it is not yet clear if 0-values describe no-flow or missing data.

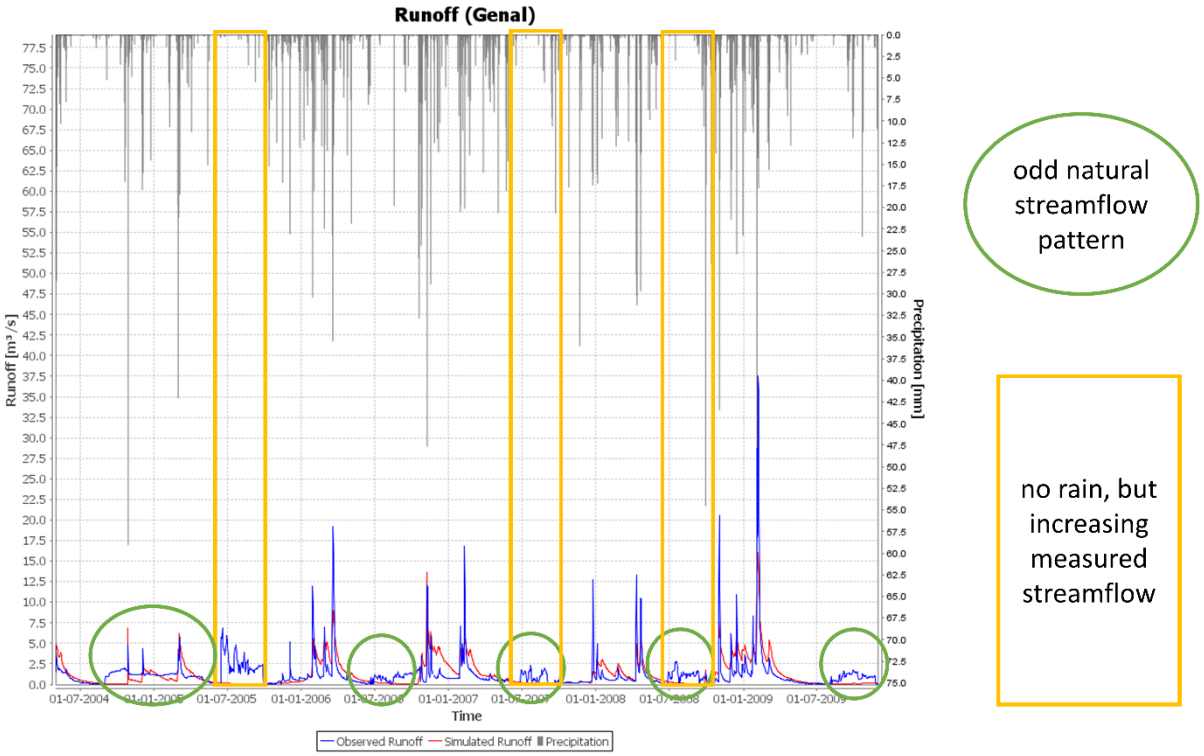

Figure 4.2: Inhomogeneity of observed streamflow data at station Jubrique in the Genal catchment (Spain).

4.2.4 Irrigation

Additional information is required for the modeling of irrigation. For example, abstracted water used for irrigation would be abstracted at a specific point and transferred to another. Depending on the location and type of irrigation, e.g. sprinkler or drip irrigation, the irrigated water would infiltrate, be used by plants, or evaporate at the new location. Observations about water abstractions were made in Genal, but no data was available about the quantity of abstracted water or exact locations of abstractions and e.g. irrigation.

In Velička, abstraction volumes were available for the last few years, but they did not explain the water imbalance in specific years or seasons. Besides, information about the type of usage (e.g. irrigation) and the exact location of the distributed water (e.g. specific HRU with arable land) were not available.

This information could also lead to a better simulation of streamflow at the reach level and prediction of flow intermittence in the future to model the pathway of the abstracted water.

4.3 Modeling of flow intermittence

Despite the successful approach of using the JAMS/J2000 hydrological model results to train the RF model to predict flow intermittence, there is not yet enough observed data in space and time to fully understand and quantify patterns of drying. For that reason, the uncertainty is significant when the trained RF is used to extrapolate the state of flow to all reaches of the DRNs. Besides, with the current database of observed flow intermittence, it is not possible to predict “pool” conditions. Therefore, we assume that we would need a few more years of data for being able to model pool states Currently, there is almost no flow intermittence data for the Croatian catchment, which prevents the training of the RF model.

The observed data contain a bias regarding the spatial representativeness of the entire river network. For example in the Finnish DRN observed data are concentrated in the Southern part of the catchment

and in the Spanish DRN, data is missing in the downstream part. Besides, more data were collected during the dry season, therefore the training dataset may be biased with an over-representation of drying events.

Several gauging stations are also affected by flow intermittence, but the use of this data can be uncertain due to unclear information on the meaning of 0-values. It was not always clear if 0-values correspond to drying events or missing values or water level below the sensor, particularly for the Hungarian DRN.

5 Conclusion

The multi-gauge, multi-objective validation of the six models showed satisfactory to good model performances for all DRNs. The modeling results were successfully used to train a Random Forest model to predict flow intermittence for five of the six DRNs.

The hydrological modeling results are available to the Dryver project members (section 6) and will continue to be updated for the duration of the project. Table 5.1 presents the provided results and short-term next steps for each DRN. The upcoming steps can be summarized in the following bullet points:

- Provision of all flow indicators from D1.1 (Künne and Kralisch 2021).
- Integration of expected data from the DRNs, for example, photo trap data from Hungary.
- Integration of provided water temperature data that could be used to increase the size of the flow intermittence datasets. However, the method to derive the states of flow from the water temperature measurements has not yet been developed for this project and should be developed in collaboration with the DRN field teams.
- Additional data retrieval of observed state of flow to implement the prediction of flow intermittence in the Butižnica DRN.
- Additional data recovery of observed flow state data during the year 2022 for all DRNs.
- Extension of the simulation to include the data from the year 2022 to have more data to train and validate the model, and thus increase the reliability of the results.

In the longer term, next steps are:

- Quantification of the hydrological model sensitivity to the parameters and calibration method.
- Evaluation of the sensitivity to predict the observed data samples used to train the RF to quantify a possible bias of these training datasets for an over-representation of drying events. For several types of observed data (ONDE stations, photo traps, citizen science), more data is collected during the dry season (section 4.3).
- Assessment of the RF model's ability to project the flow states under future climatic scenarios (in collaboration with Task 1.3)

Table 5.1: Summary of the provided results and next steps

DRN	Provided results (period of simulation : 2005-10-01 to 2021-09-30)	Next steps
Albarine	• Simulated daily discharge for each reach • Simulated daily state of flow for each reach	• Integrate data from water temperature loggers • Retrieve available observed flow intermittence data from DRN team for the year 2022 • Extend the simulation results up to 2022-09-30 • Provide all flow indicators
Bukkosdi	• Simulated daily discharge for each reach • Simulated daily state of flow for each reach	• Integrate data from photo traps and water temperature loggers • Retrieve available observed flow intermittence data from DRN team for the year 2022 • Extend the simulation results up to 2022-09-30 • Provide all flow indicators
Butižnica	• Simulated daily discharge for each reach	• Retrieve more observed flow intermittence to simulate the flow conditions in the DRN • Extend the simulation results up to 2022-09-30 for discharge
Genal	• Simulated daily discharge for each reach • Simulated daily state of flow for each reach	• Integrate data from water temperature loggers • Retrieve available observed flow intermittence data from DRN team for the year 2022 • Extend the simulation results up to 2022-09-30 • Provide all flow indicators
Lepsämänjoki	• Simulated daily discharge for each reach • Simulated daily state of flow for each reach	• Integrate data from water temperature loggers • Retrieve available observed flow intermittence data from DRN team for the year 2022 • Extend the simulation results up to 2022-09-30 • Provide all flow indicators
Velička	• Simulated daily discharge for each reach • Simulated daily state of flow for each reach	• Retrieve available observed flow intermittence data from DRN team for the year 2022 • Extend the simulation results up to 2022-09-30 • Provide all flow indicators

6 Shared data and results

Data, models, parameter values, flow indicators, and simulated results are accessible to all DRYvER members on the shared Teams repository here (in WP1 - Hydrological trajectories of DRNs/Results).

The JAMS/J2000 models and RF models for each DRN can be found in the “models” folder.

The “data” folder contains for each DRN :

- a shapefile with the river network used for the hydrological modeling,
- a pdf file describing the method used for the generation of the river networks and explaining the main differences between the generated river network and the reference river network provided by the DRNs,
- a shapefile with the outline of the small catchment
- the observed flow intermittence data used to train and validate the Random Forest model
- the results of the hydrological modeling for the present period (2005 - 2021) (for more detailed description see below)
- the flow indicators 1 to 11 as defined in the deliverable 1.1 (Künne and Kralisch 2021)

- a zip-file containing the JAMS “dryver_indices.jam” component to calculate the flow indicators defined in the deliverable 1.1 as well as the JAMS data explorer for further spatio-temporal analysis of the flow intermittence indicators

The results are shared as netcdf files containing (i) the discharges and baseflow simulated with the JAMS/J2000 models in m^3/s, (ii) the probability of a flowing event, and (iii) the state of flow (dry or flowing) at daily time step for all the DRN reaches.

An R script is provided to open the netcdf files, display the river networks and extract time series for specific reaches. It also provides an example for computing indicators of flow intermittence and displaying the results.

More information regarding the shared models and data can be found in the README.txt file.

The models and results may be updated during the next months. All information regarding these updates will be provided in the “Results” folder.

Access to models, data, and results is currently restricted to the members of the DRYvER project, and will be made publicly available at a later date. Meanwhile, data can be shared with people outside the DRYvER project on request.

References

Ad-hoc-AG Boden (2005) Bodenkundliche Kartieranleitung, 5th edn. Hannover

Allen RG, Pereira LS, Raes D, Smith M (1998) Crop Evapotranspiration (guidelines for computing crop water requirements). FAO Irrig Drain Pap 300:300. https://doi.org/10.1016/j.eja.2010.12.001

Andreas G, Duscher K (2019) Extended vector data of the International Hydrogeological Map of Europe 1:1,500,000 (Version IHME1500 v1.2). 13

Beaufort A, Carreau J, Sauquet E (2019) A classification approach to reconstruct local daily drying dynamics at headwater streams. Hydrol Process 33:1896–1912. https://doi.org/10.1002/hyp.13445

BGR E& U (2013) International Hydrogeological Map of Europe, scale 1:1, 500, 000

Branger F, Gouttevin I, Tilmant F, Cipriani T, Barachet C, Gros C Le, Sauquet E, Braud I, Leblois E, Branger F, Gouttevin I, Tilmant F, Cipriani T, Barachet C (2016) Modélisation hydrologique distribuée du Rhône To

Breimann L (2001) Random Forests. Mach Learn 45:5–32

Copernicus Land Monitoring Service (2020) Corine Land Cover (CLC) 2012, Version 2020_20u1

Copernicus Land Monitoring Service (2016) European Digital Elevation Model (EU-DEM), version 1.1. https://land.copernicus.eu/imagery-in-situ/eu-dem/eu-dem-v1.1/view. Accessed 10 Apr 2021

Cornes RC, van der Schrier G, van den Besselaar EJM, Jones PD (2018) An Ensemble Version of the E-OBS Temperature and Precipitation Data Sets. J Geophys Res Atmos 123:9391–9409. https://doi.org/10.1029/2017JD028200

Cucchi M, P. Weedon G, Amici A, Bellouin N, Lange S, Müller Schmied H, Hersbach H, Buontempo C (2020) WFDE5: Bias-adjusted ERA5 reanalysis data for impact studies. Earth Syst Sci Data 12:2097–2120. https://doi.org/10.5194/essd-12-2097-2020

Datry T, Allen D, Argelich R, Barquin J, Bonada N, Boulton A, Branger F, Cai Y, Cañedo-Argüelles M, Cid N, Csabai Z, Dallimer M, de Araújo JC, Declerck S, Dekker T, Döll P, Encalada A, Forcellini M, Foulquier A, Heino J, Jabot F, Keszler P, Kopperoinen L, Kralisch S, Künne A, Lamouroux N, Lauvernet C, Lehtoranta V, Loskotová B, Marcé R, et al (2021) Securing Biodiversity, Functional Integrity, and Ecosystem Services in Drying River Networks (DRYvER). Res Ideas Outcomes 7:. https://doi.org/10.3897/rio.7.e77750

Deb K, Member A, Pratap A, Agarwal S, Meyarivan T (2002) A Fast and Elitist Multiobjective Genetic Algorithm: NSGA-II. 6:182–197

FAO (2006) Guidelines for Soil Description. Food and Agriculture Organization of the United States, Rome

Faroux S, Kaptué Tchuenté AT, Roujean J-L, Masson V, Martin E, Le Moigne P (2013) ECOCLIMAP-II/Europe: a twofold database of ecosystems and surface parameters at 1 km resolution based on satellite information for use in land surface, meteorological and climate models. Geosci Model Dev 6:563–582. https://doi.org/10.5194/gmd-6-563-2013

Fink M, Krause P, Kralisch S, Bende-Michl U, Flügel WA (2007) Development and application of the modelling system J2000-S for the EU-water framework directive. Adv Geosci 11:123–130. https://doi.org/10.5194/adgeo-11-123-2007

Flügel W-A (1996) Hydrological response units (HRU's) as modelling entities for hydrological river basin simulation and their methodological potential for modelling complex environmental process systems. Results from the Sieg catchment. Erde 127:43–62

González-Ferreras AM, Barquín J (2017) Mapping the temporary and perennial character of whole river networks. Water Resour Res 53:6709–6724. https://doi.org/10.1002/2017WR020390

Gouttevin I, Turko M, Branger F, Leblois E, Sicart JE (2017) Snow 2016-2017: Improvement of distributed hydrological modelling in natural conditions in the Alps.

GSOD Global Surface Summary of the Day - GSOD. National Climatic Data Center, NESDIS, NOAA, U.S. Department of Commerce

Gupta H V., Kling H, Yilmaz KK, Martinez GF (2009) Decomposition of the mean squared error and NSE performance criteria: Implications for improving hydrological modelling. J Hydrol 377:80–91. https://doi.org/10.1016/j.jhydrol.2009.08.003

Hall DK, Riggs GA (2016) MODIS/Terra Snow Cover 8-Day L3 Global 500m SIN Grid, Version 6. In: Boulder, Color. USA. NASA Natl. Snow Ice Data Cent. Distrib. Act. Arch. Cent. https://nsidc.org/data/mod10a2. Accessed 17 Sep 2021

Hartmann A (2013) Modeling karst hydrology and hydrochemistry at different scales and in different climates considering uncertainty. Inst Hydrol PhD:

Kralisch S, Krause P (2006) JAMS - A Framework for Natural Resource Model Development and Application. In: 7th International Conference on Hydroinformatics. Nice, France, p 6

Krause P (2001) Das hydrologische Modellsystem J2000. Beschreibung und Anwendung in großen Flussgebieten. Jülich

Krause P (2002) Quantifying the impact of land use changes on the water balance of large catchments using the {J}2000 model. Phys Chem Earth, Parts A/B/C 27:663–673. https://doi.org/10.1016/S1474-7065(02)00051-7

Kundzewicz ZW, Krysanova V, Benestad RE, Hov, Piniewski M, Otto IM (2018) Uncertainty in climate change impacts on water resources. Environ Sci Policy 79:1–8. https://doi.org/10.1016/j.envsci.2017.10.008

Künne A, Kralisch S (2021) Report on flow intermittence indicators

Legates DR, McCabe Jr GJ (1999) Evaluating the use of "goodness-of-fit" measures in hydrologic and hydroclimatic model validation. Water Resour Res 35:233–241

Liaw A, Wiener M (2002) Classification and Regression by randomForest. R News 2:18–22

Llorente M, Rovira P, Merino A, Rubio A, Turrión M, Badía D, Romanya J, González JCJA (2018) The CARBOSOL Database: a georeferenced soil profile analytical database for Spain. PANGAEA. https://doi.org/https://doi.org/10.1594/PANGAEA.884517

Ludwig K, Bremicker M (2006) The Water Balance Model LARSIM: Design, Content and Applications, Freiburger. Förderverein Hydrologie an der Albert-Ludwigs-Universität Freiburg im Breisgau, Freiburg

Messager ML, Lehner B, Cockburn C, Lamouroux N, Pella H, Snelder T, Tockner K, Trautmann T, Watt C, Datry T (2021) Global prevalence of non-perennial rivers and streams. Nature 594:391–397. https://doi.org/10.1038/s41586-021-03565-5

Mimeau L, Künne A, Kralisch S, Branger F, Vidal J (2022) Inter-comparison of climatological datasets

for the hydrological modelling of six european catchments. 869226

Moriasi DN, Arnold JG, Van Liew MW, Bingner RL, Harmel RD, Veith TL (2007) Model Evaluation Guidelines for Systematic Quantification of Accuracy in Watershed Simulations. Trans ASABE 50:885–900. https://doi.org/10.13031/2013.23153

Muñoz-Sabater J, Dutra E, Agustí-Panareda A, Albergel C, Arduini G, Balsamo G, Boussetta S, Choulga M, Harrigan S, Hersbach H, Martens B, Miralles D, Piles M, Rodríguez-Fernández N, Zsoter E, Buontempo C, Thépaut J-N (2021) ERA5-Land: A state-of-the-art global reanalysis dataset for land applications. Earth Syst Sci Data Discuss 1–50. https://doi.org/10.5194/essd-2021-82

Neitsch SL, Arnold JG, Kiniry JR, Williams JR (2011) Soil & Water Assessment Tool Theoretical Documentation Version 2009. Texas Water Resour Inst 1–647. https://doi.org/10.1016/j.scitotenv.2015.11.063

Panagos P, Van Liedekerke M, Jones A, Montanarella L (2012) European Soil Data Centre: Response to European policy support and public data requirements. Land use policy 29:329–338. https://doi.org/10.1016/j.landusepol.2011.07.003

Pfennig B, Kipka H, Wolf M, Fink M, Krause P, Flügel W-A (2009) Development of an extended routing scheme in reference to consideration of multi-dimensional flow relations between hydrological model entities. 1972–1978

Szalai S, Auer I, Hiebl J, Milkovich J, Radim T, Stepanek P, Zahradnicek P, Bihari Z, Lakatos M, Szentimrey T, Limanowka D, Kilar P, Cheval S, Deak G, Mihic D, Antolovic I, Mihajlovic V, Nejedlik P, Stastny P, Mikulov J (2013) Climate of the Greater Carpathian Region

U.S. Geological Survey (2015) Shuttle Radar Topography Mission (SRTM)

van Meerveld HJI, Kirchner JW, Vis MJP, Assendelft RS, Seibert J (2019) Expansion and contraction of the flowing stream network alter hillslope flowpath lengths and the shape of the travel time distribution. Hydrol Earth Syst Sci 23:4825–4834. https://doi.org/10.5194/hess-23-4825-2019

Vidal J-P, Martin E, Franchistéguy L, Baillon M, Soubeyroux J-M (2010) A 50-year high-resolution atmospheric reanalysis over France with the Safran system. Int J Climatol 30:1627–1644. https://doi.org/10.1002/joc.2003

Watson A, Kralisch S, Künne A, Fink M, Miller J (2020) Impact of precipitation data density and duration on simulated flow dynamics and implications for ecohydrological modelling in semi-arid catchments in Southern Africa. J Hydrol 590:125280. https://doi.org/10.1016/j.jhydrol.2020.125280

Watson A, Kralisch S, van Rooyen J, Miller J (2021) Quantifying and understanding the source of recharge for alluvial systems in arid environments through the development of a seepage model. J Hydrol 601:126650. https://doi.org/10.1016/j.jhydrol.2021.126650

Appendix

A.1 River networks

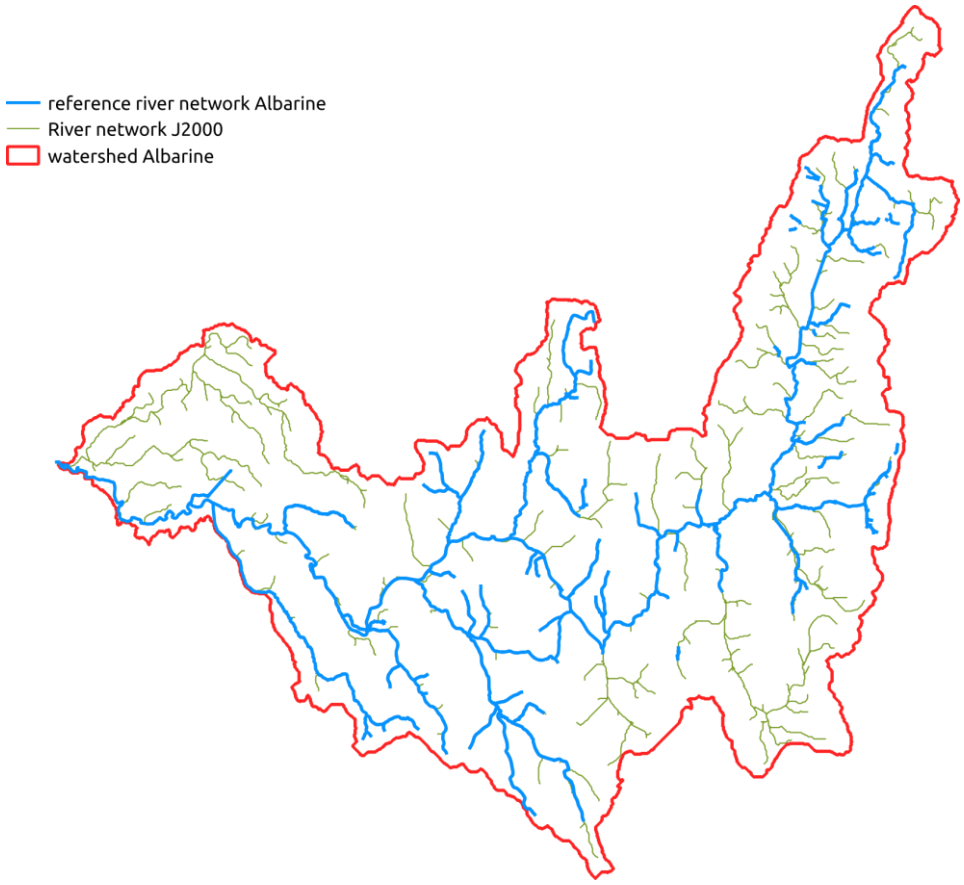

Figure A1.1: Generated (green) and reference (blue) river networks for the Albarine catchment

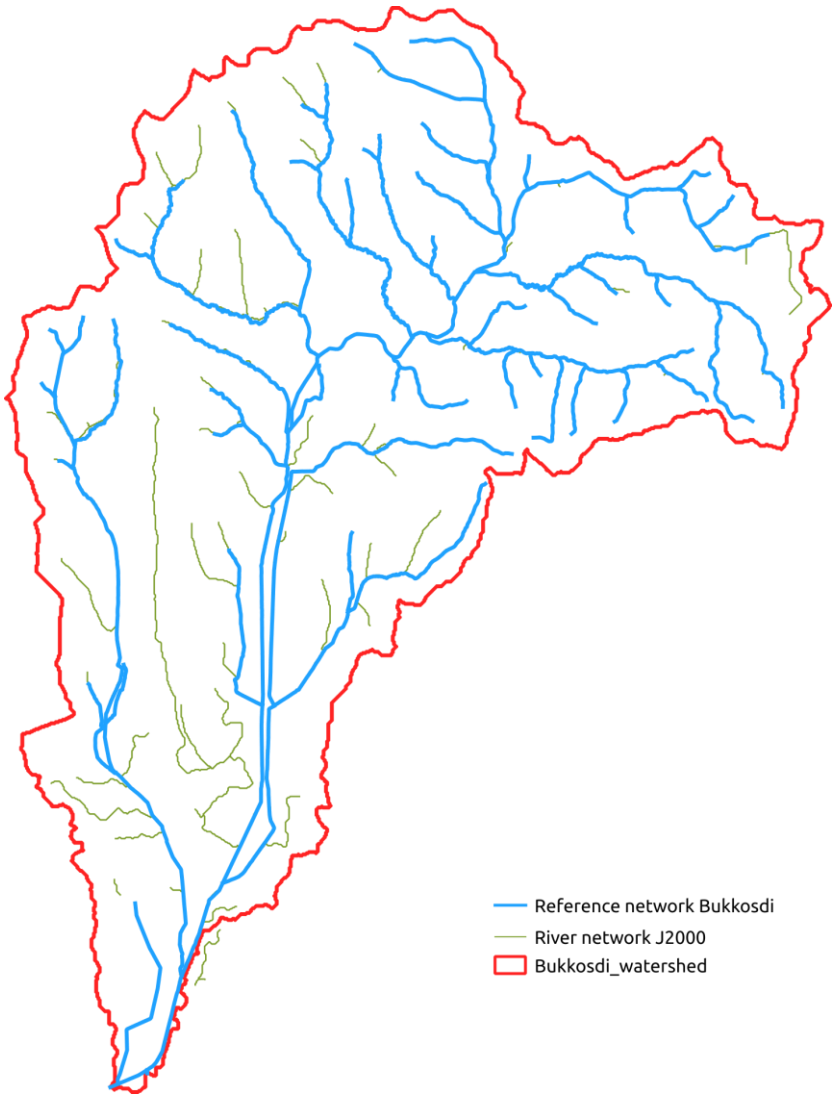

Figure A1.2: Generated (green) and reference (blue) river networks for the Bukkosdi catchment

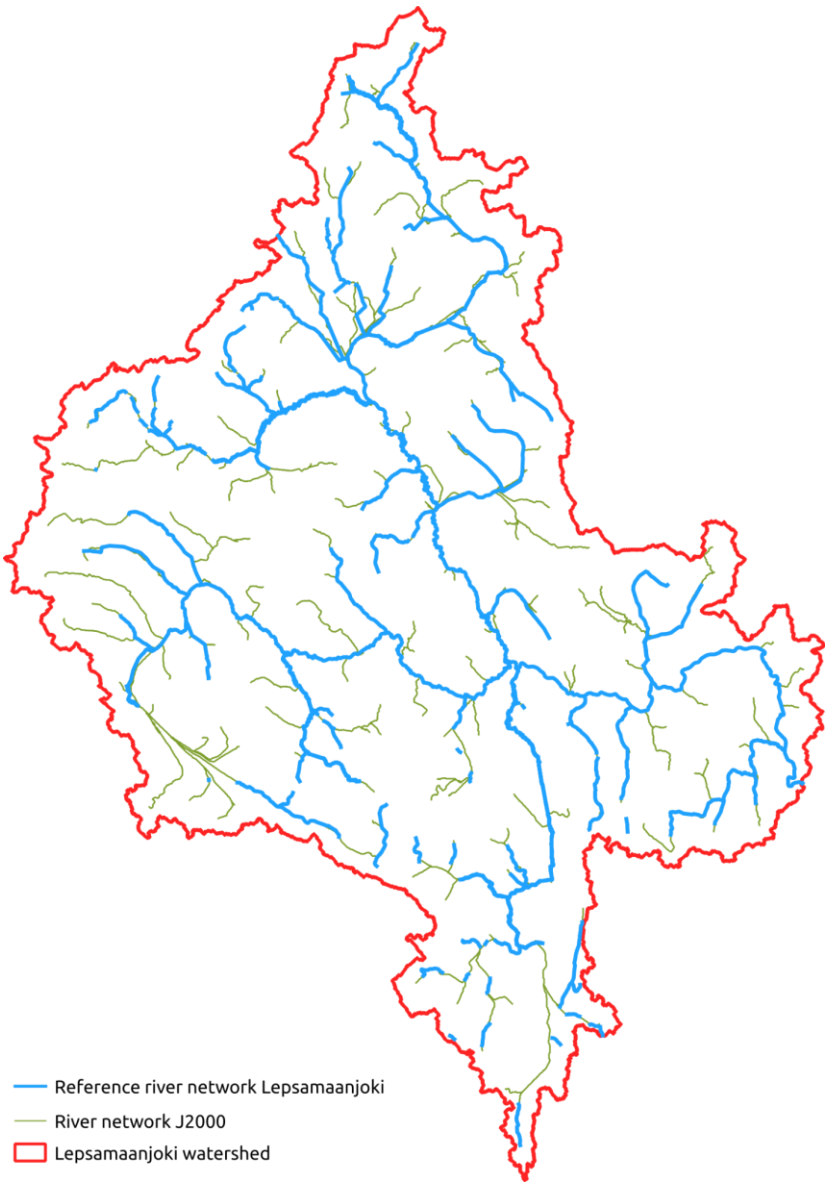

Figure A1.3: Generated (green) and reference (blue) river networks for the Lepsämänjoki catchment

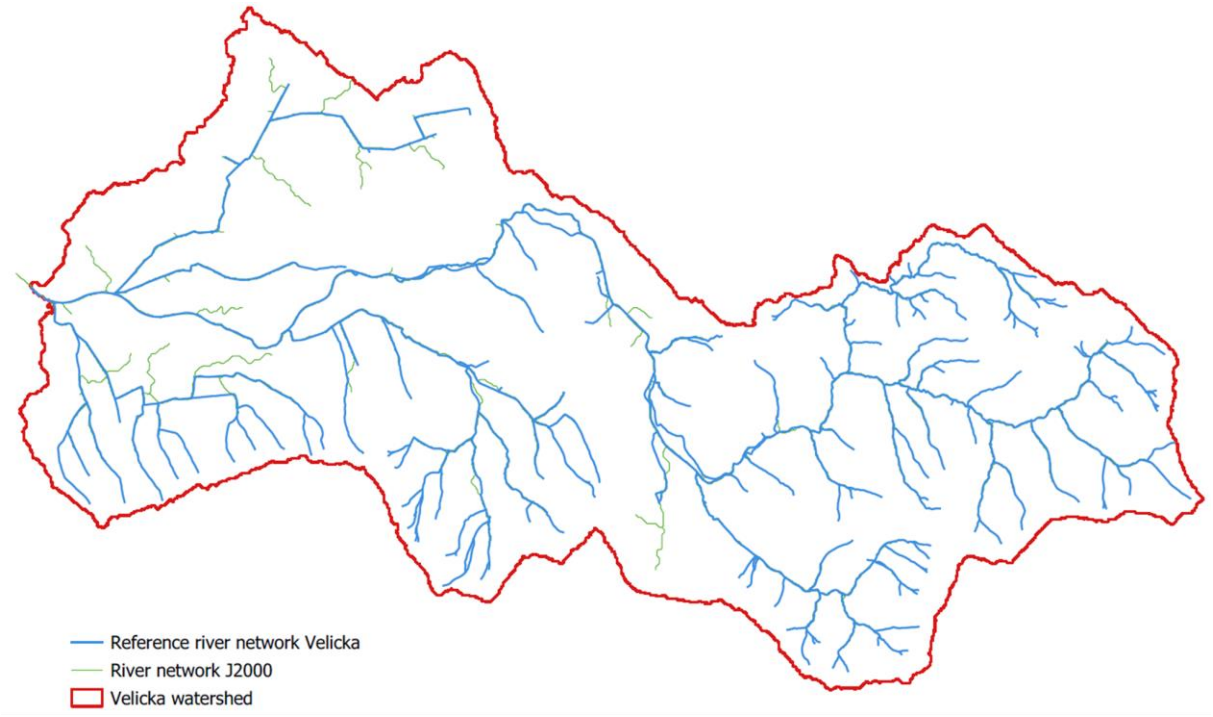

Figure A1.4: Generated (green) and reference (blue) river networks for the Veličká catchment

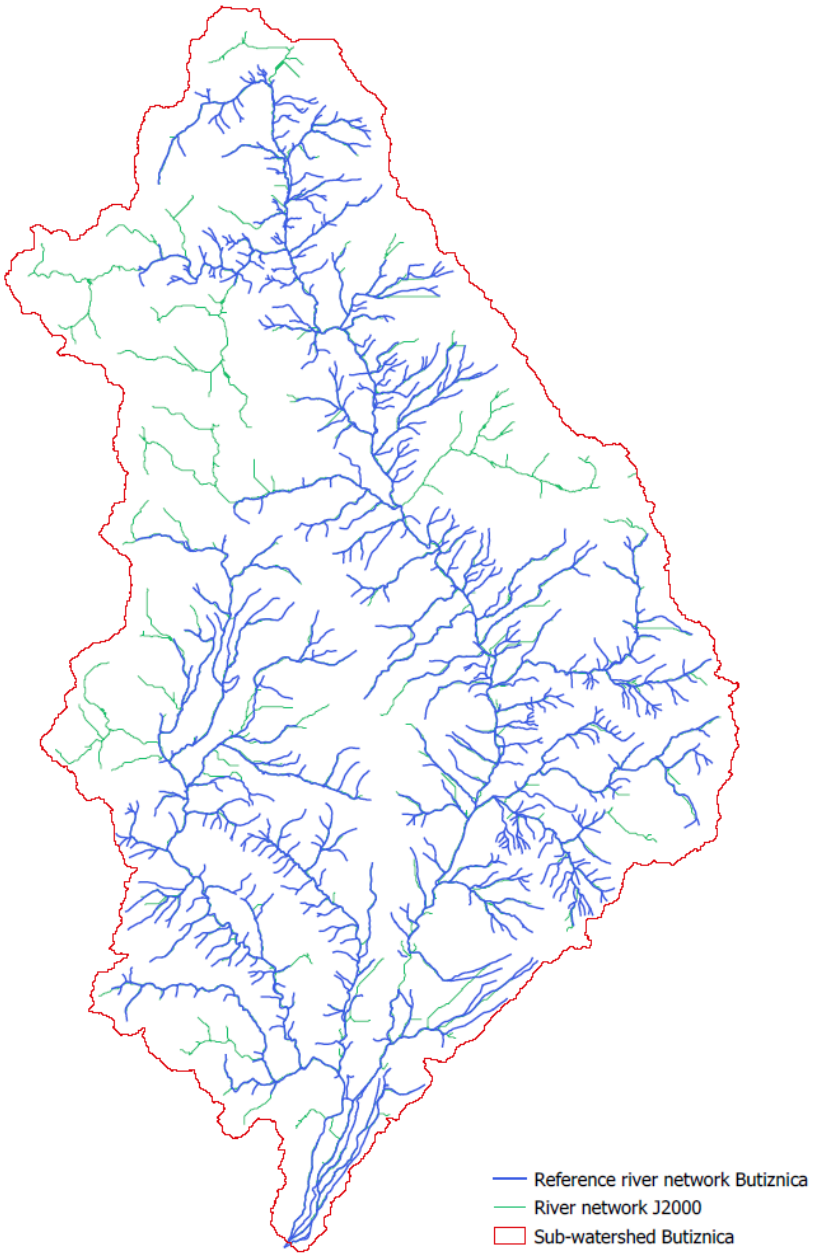

Figure A1.5: Generated (green) and reference (blue) river networks for the Butižnica catchment

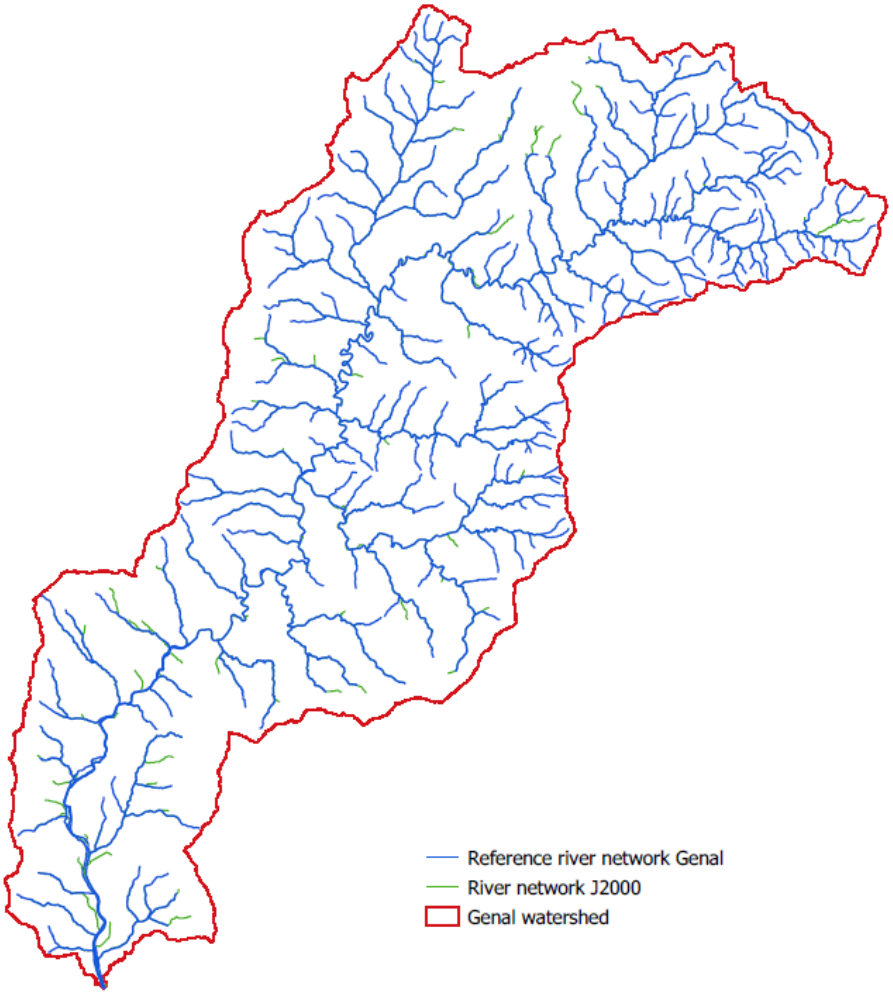

Figure A1.6: Generated (green) and reference (blue) river networks for the Genal catchment

A.2 HRU Delineation

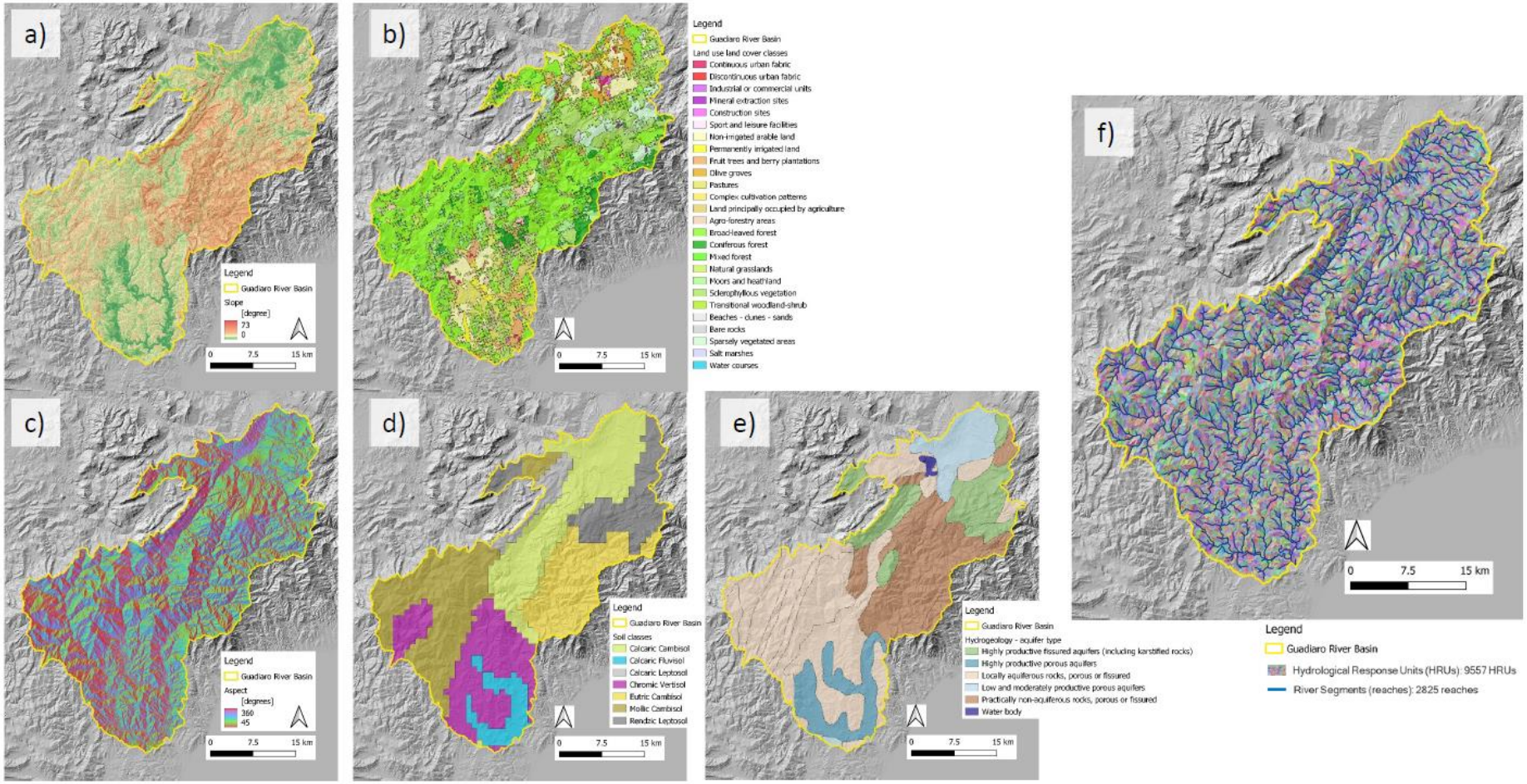

Figure A2.1: Classes of slope (a), LULC (b), aspect (c), soil types (d) and hydro-geology (e) were used as inputs and resulted in the final modeling entities (f) used for modeling hydrological processes at each Hydrological Response Units as well as aggregated runoff processes at the sub-catchments/ reach level. For Guadiaro this resulted in 9,557 HRUs and 2,825 reaches.

A.3 Calibrated parameters

Table A1: List of the calibrated parameters and the calibration range

Abbreviation	Description	Unit	Type	Calibration range		
				Ain, Vantaanjoki	Fekete	Guadiaro, Krka, Morava
snow_trans	Half width of the transition zone rainfall-snowfall	K	global	0 - 3.5		
snow_trs	Threshold temperature for precip phase (the temp. in which 50 % of precip fall as snow and 50 % as rain)	°C	global	0 - 3		
t_factor	Temperature factor for snow melt	$mm*°C^{-1}$	global	0 - 8		
ccf_factor	Cold content factor	-	global	0.0001 - 0.01		
CropCoef_aAF	Crop coefficient additive adaptation factor	-	global	-0.2 - 0.2		
CropCoef_mAF	Crop coefficient multiplicative adaptation factor	-	global	0.5 - 2		
FCAdaptation	Multiplier for field capacity	-	global	0.5 - 5	0.5 - 7	0.5 - 3
ACAdaptation	Multiplier for air capacity	-	global	0 - 3	0 - 3	0.5 - 3
soilPolRed	Polynomic reduction factor for potential evapotranspiration	-	global	0 - 10		
soilMaxInfSnow	Maximum infiltration for snow covered areas	mm	global	5 - 200		
soilMaxInfSummer	Maximum infiltration in summer (Apr - Sep)	mm	global	5 - 200		
soilMaxInfWinter	Maximum infiltration in winter (Oct - Mar)	mm	global	5 - 200		
soilMaxPerc	Maximum percolation rate	mm	global	1 - 20		
soilLatVertLPS	LPS lateral-vertical distribution coefficient	-	global	0 - 10		
soilOutLPS	LPS outflow coefficient	-	global	0 - 10		
SoilConcRD1	Recession coefficient for surface runoff	-	global	1 - 5		1 - 10

SoilConcRD2	Recession coefficient for interflow	-	global	1 - 10		
gwRG1RG2dist	Distribution factor between shallow and deep groundwater aquifer	-	global	0 - 10		
flowRouteTA	Flow routing coefficient TA	-	global	1 - 20		1 -30
RG1_max	Maximum storage capacity of the upper ground-water reservoir	mm	spatially distributed	10 - 300		not calibrated
RG1_k	Storage coefficient of the upper ground-water reservoir	d	spatially distributed	2 - 30		0.3 – 3-times of physically determined parameter
RG2_max	Maximum storage capacity of the lower ground-water reservoir	mm	spatially distributed	100 - 1500	100 - 1000	not calibrated
RG2_k	Storage coefficient of the lower ground-water reservoir	d	spatially distributed	10 - 600	10 - 650	0.3 – 3-times of physically determined parameter

A.4 Snow calibration

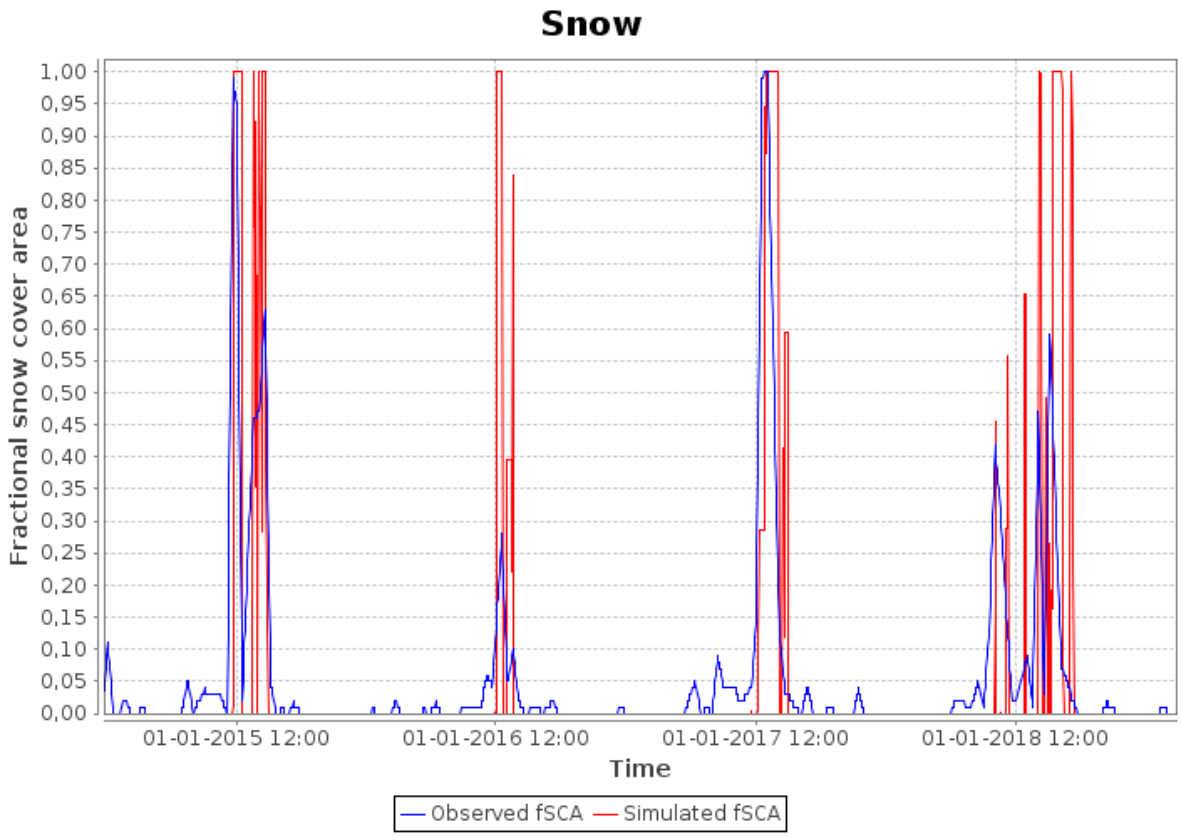

Figure A5: Simulated (red) and observed (blue) snow cover area (fSCA) for the Fekete catchment

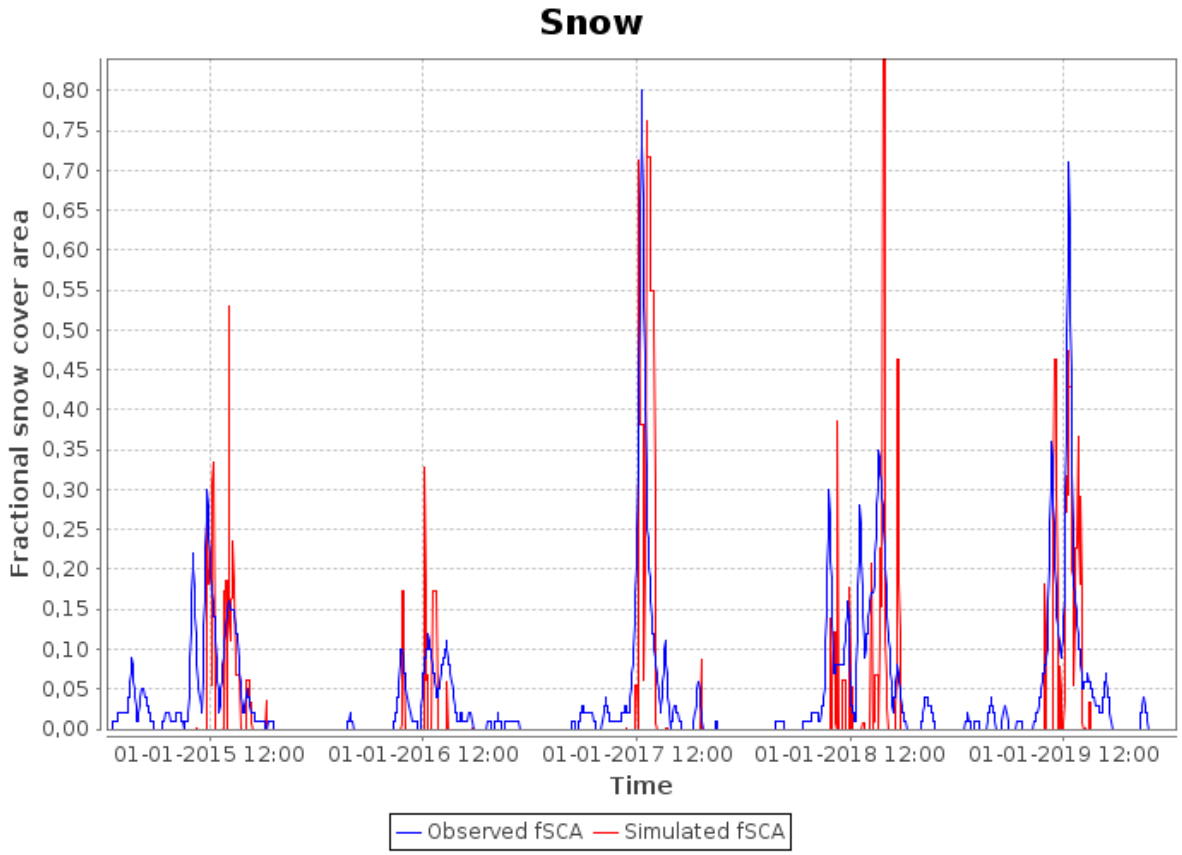

Figure A6: Simulated (red) and observed (blue) snow cover area (fSCA) for the Krka catchment

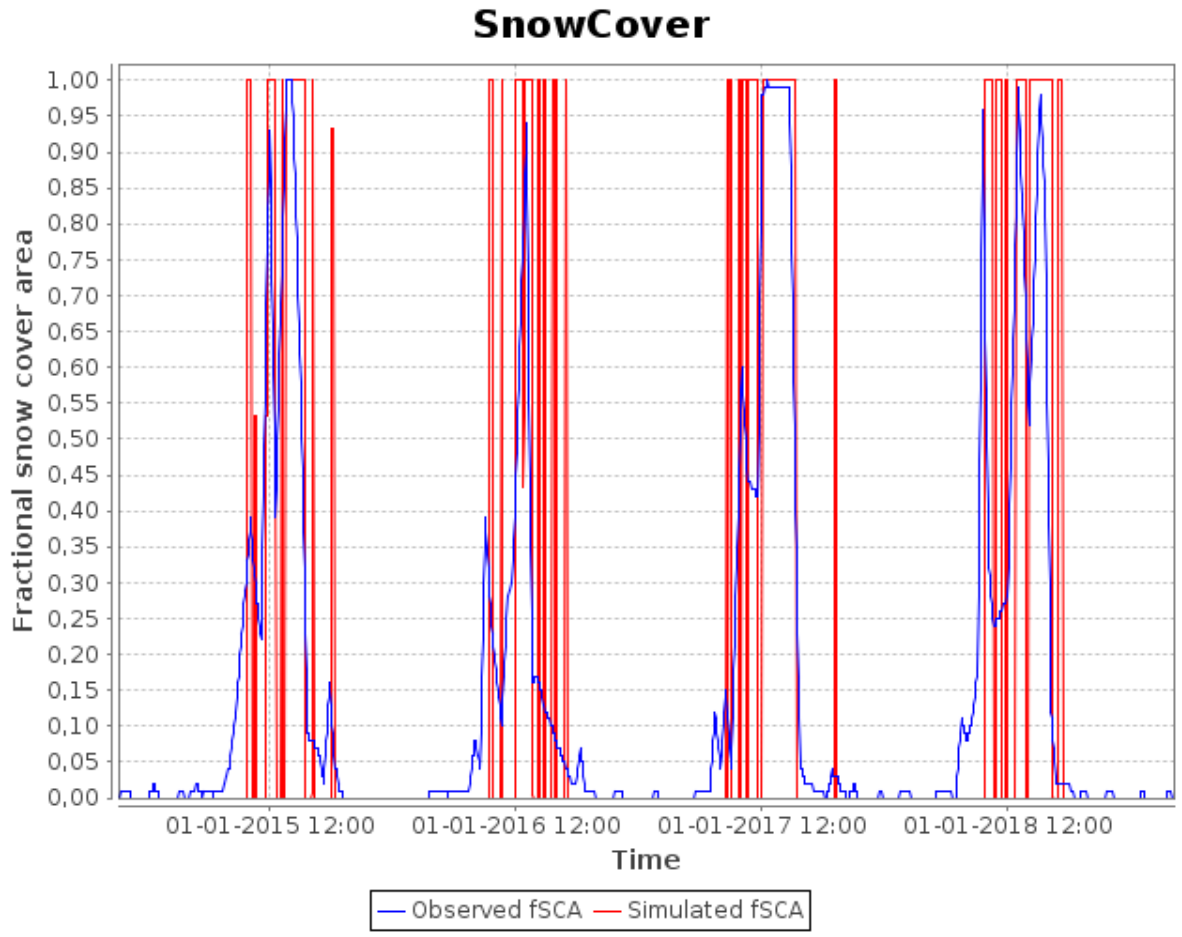

Figure A7: Simulated (red) and observed (blue) snow cover area (fSCA) for the Morava catchment

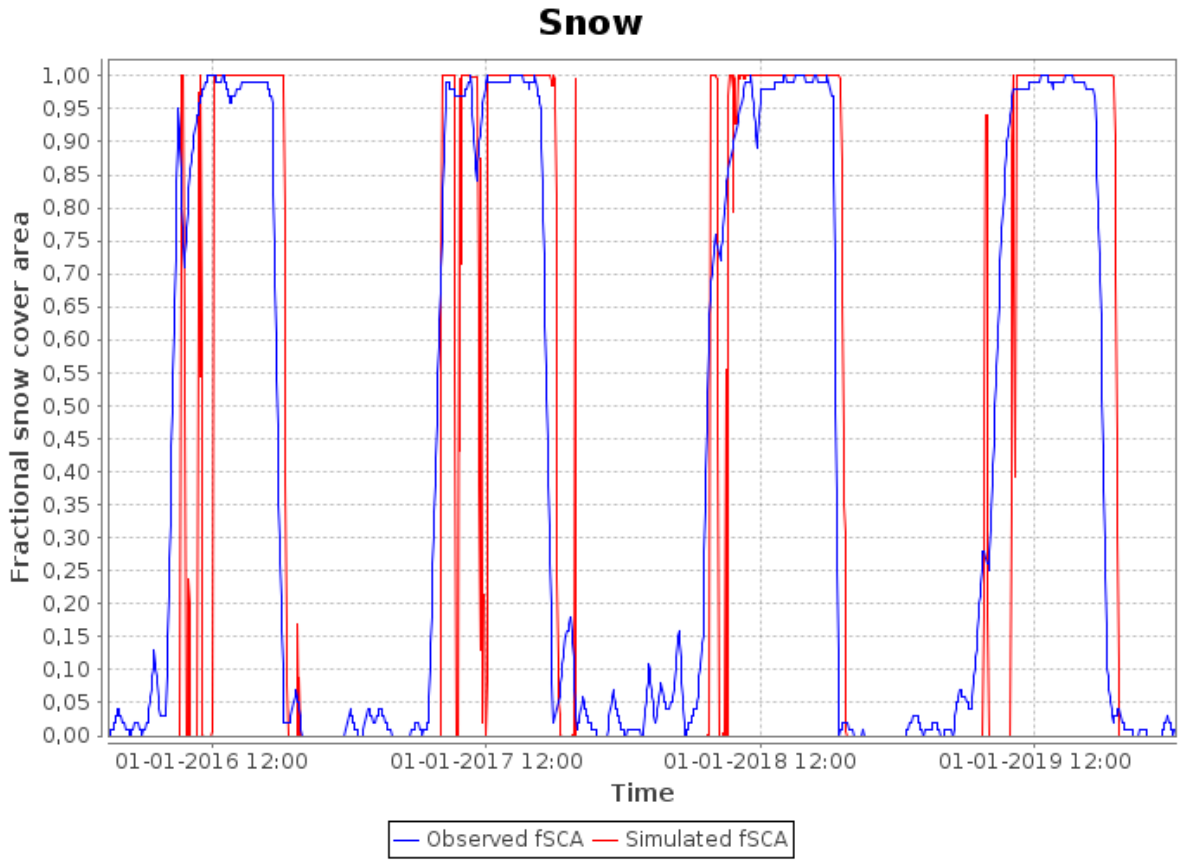

Figure A8: Simulated (red) and observed (blue) snow cover area (fSCA) for the Vantaanjoki catchment

A.5 Hydrogeology

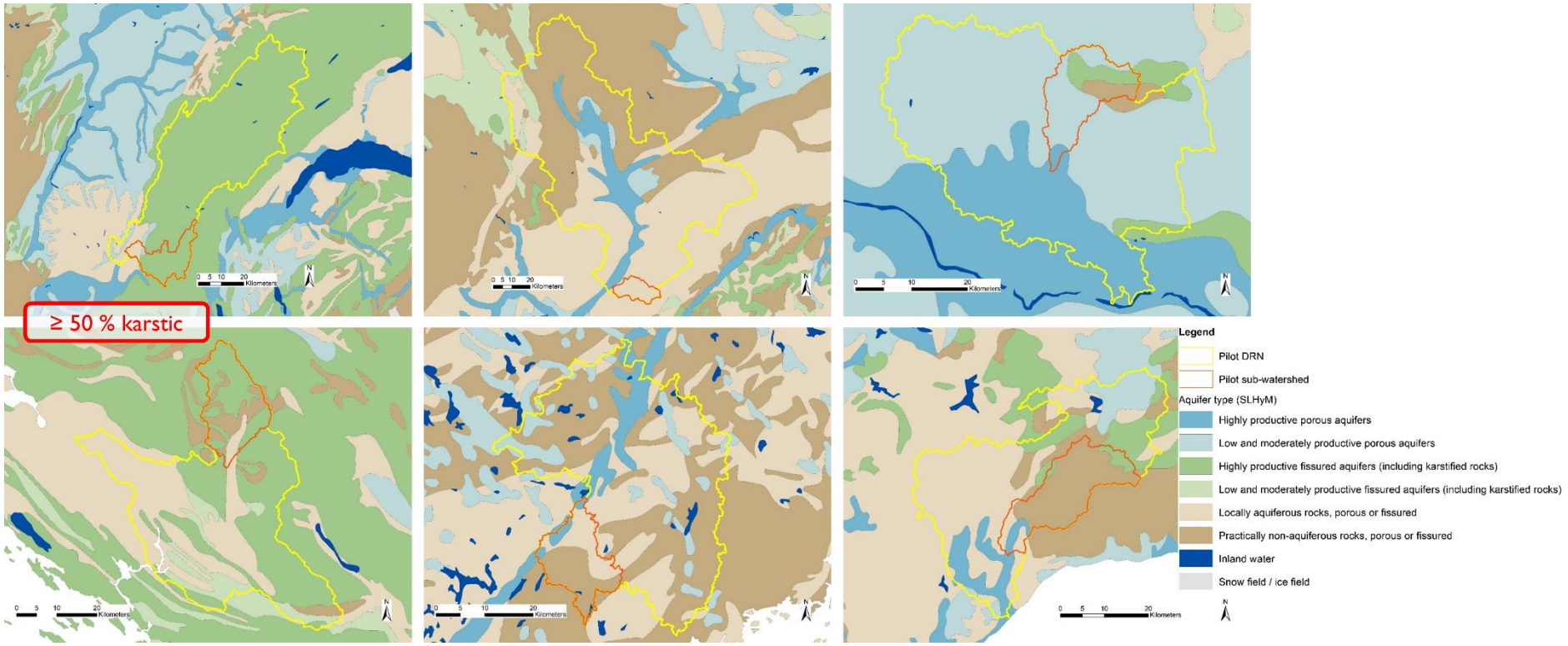

Figure A9: Aquifer types of the six DRNs. The light and dark green areas represent karstified rocks, which play a role in four out of the six basins and account for around 50% and more in the Croatian and French catchment